Biochemical Pharmacology 81 (2011) 761–776

Contents lists available at ScienceDirect

Biochemical Pharmacology

journal homepage: www.elsevier.com/locate/biochempharm

In vitro liver metabolism of aclidinium bromide in preclinical animal species and humans: Identification of the human enzymes involved in its oxidative metabolism

Joan J. Albertí *, Sònia Sentellas, Miquel Salvà

Department of Pharmacokinetics and Drug Metabolism, Almirall, S.A., Laureà Miró 408-410, 08980 Sant Feliu de Llobregat, Barcelona, Spain

ARTICLE INFO

Article history:
Received 28 October 2010
Accepted 10 December 2010
Available online 22 December 2010

Keywords:
Aclidinium bromide
In vitro metabolism
Interspecies differences
Enzyme identification

ABSTRACT

The metabolism of aclidinium bromide, a novel long-acting antimuscarinic drug for the maintenance treatment of chronic obstructive pulmonary disorder, has been investigated in liver microsomes and hepatocytes of mice, rats, rabbits, dogs, and humans. Due to the rapid hydrolysis of this ester compound, two distinct radiolabeled forms of aclidinium were studied. The main biotransformation route of aclidinium was the hydrolytic cleavage of the ester moiety, resulting in the formation of the alcohol metabolite (M2, LAS34823) and carboxylic acid metabolite (m3, LAS34850), which mainly occurred non-enzymatically. By comparison, the oxidative metabolism was substantially lower and the metabolite profiles were similar across all five species examined. Aclidinium was metabolized oxidatively to four minor primary metabolites that were identified as monohydroxylated derivatives of aclidinium at the phenyl (M4) and glycolyl (m6 and m7) moieties of the molecule. The NADPH-dependent metabolite m4 involved the loss of one of the thiophene rings of aclidinium. Incubations with human recombinant P450 isoforms and inhibition studies with selective chemical inhibitors and antibodies of human P450 enzymes demonstrated that the oxidative metabolism of aclidinium is primarily mediated by CYP3A4 and CYP2D6. Additionally, up to eight secondary metabolites were also characterized, involving further hydrolysis, oxidation, or glucuronidation of the primary metabolites. Also, the liver oxidative metabolism of the alcohol metabolite (LAS34823) resulted in the production of one hydroxylated metabolite (M1) mediated by human CYP2D6, whereas the acid metabolite (LAS34850) was not metabolized enzymatically, although a minor non-enzymatic and NADPH-dependent reduction was observed.

1. Introduction

Aclidinium bromide (AB) (also known as 3R-(2-hydroxy-2,2-dithiophen-2-yl-acetoxy)-1-(3-phenoxy-propyl)1-azonia bicyclo [2.2.2] octane bromide) is a novel, long-acting muscarinic antagonist [1] undergoing Phase III clinical trials for the maintenance treatment of chronic obstructive pulmonary disorder. This ester compound displayed non-enzymatic hydrolysis of its ester bond at neutral and basic pH. Furthermore, AB was rapidly hydrolyzed in plasma of different animal species and humans to yield its alcohol (LAS34823) and carboxylic acid (LAS34850) metabolites [2,3]. The main human esterase involved in the enzymatic hydrolysis of aclidinium was identified as butyrylcholinesterase (BChE), which is found mainly in human plasma. Cytochrome P450-catalyzed ester cleavage was not observed in human liver microsomes [4].

In vitro incubations with liver microsomes and/or hepatocytes can be used to predict potential biotransformations in humans and in those animal species used for preclinical safety studies. Hepatocyte incubations retain Phase I and Phase II enzyme activities and are therefore useful in determining overall metabolism. They also mimic in vivo metabolism more accurately than incubations with subcellular fractions [5]. Previous data using diagnostic substrates have shown that P450 activities in rat, dog, monkey, and human hepatocyte suspensions are not significantly decreased by cryopreservation [6].

The objectives of this study were (a) to compare the in vitro metabolism of aclidinium in liver microsomes and hepatocytes of different preclinical animal species and humans; (b) to identify the oxidative metabolites; and (c) to identify and kinetically characterize the human enzymes responsible for the oxidative

Abbreviations: AB, aclidinium bromide; BChE, butyrylcholinesterase; CID, collision-induced dissociation; P450, cytochrome P450; ESI, electrospray ionization; FMO, flavin-containing monooxigenases; glyc, glycolyl; K_h, hydrolysis rate constant; LC, liquid chromatography; MRM, multiple reaction monitoring; MS, mass spectrometry; *m/z*, mass-to-charge ratio; phe, phenyl; SPE, solid-phase extraction; TEA, triethylamine.

* Corresponding author. Tel.: +34 93 291 29 48; fax: +34 93 291 29 97.
E-mail address: joan.alberti@almirall.com (J.J. Albertí).

0006-2952/$ – see front matter © 2010 Elsevier Inc. All rights reserved.
doi:10.1016/j.bcp.2010.12.013

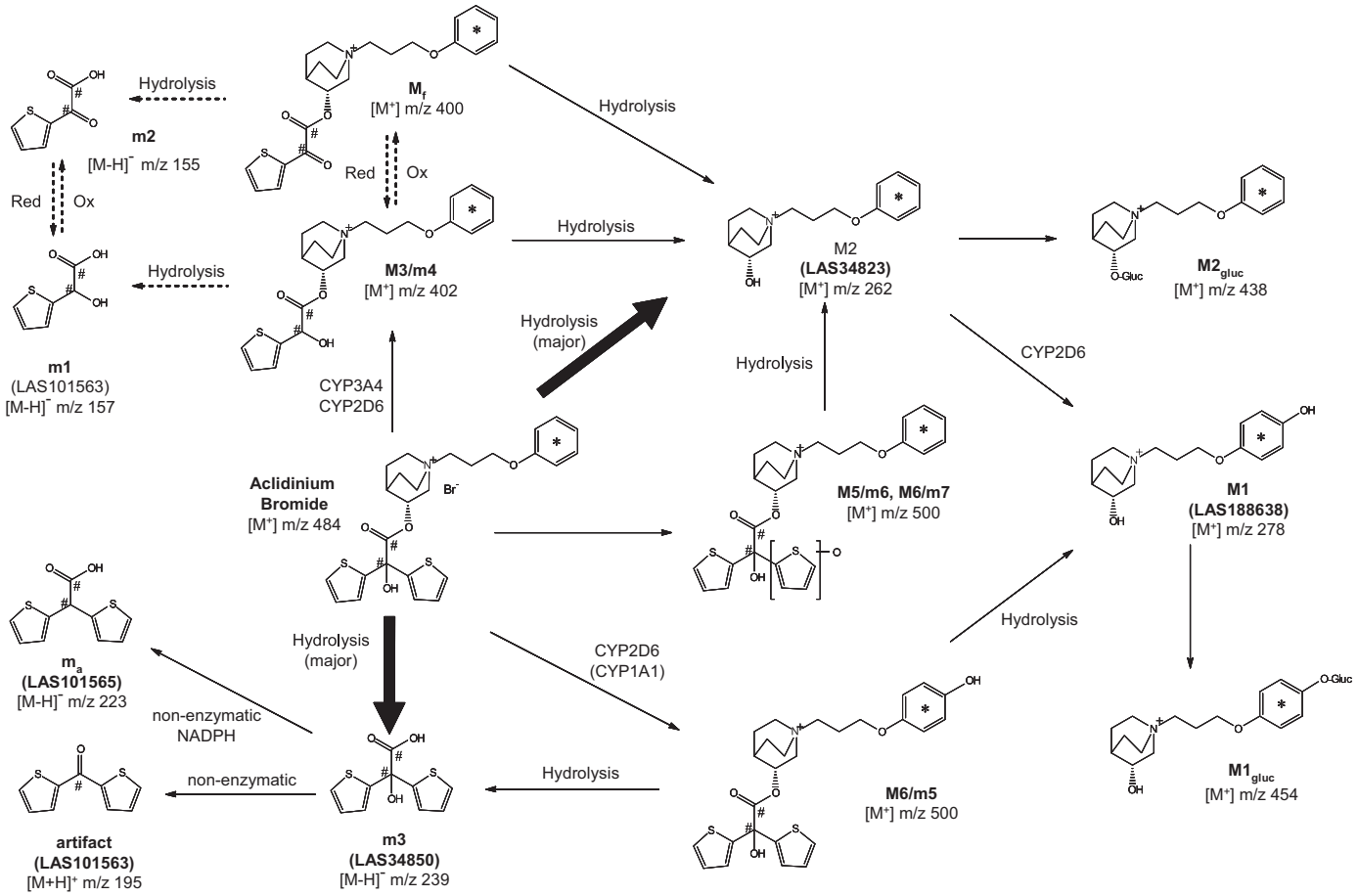

Fig. 1. Proposed in vitro metabolic pathways for aclidinium bromide in animal species and humans. Dashed arrows indicate possible paths of metabolite formation. Symbols * and # denote the positions of ^{14}C-labeled carbon atoms in ^{14}C-phe-AB and ^{14}C-glyc-AB, respectively. Metabolites generated from ^{14}C-phe-AB incubations were coded as "M", whereas metabolites generated from ^{14}C-glyc-AB incubations were coded as "m".

metabolism. Due to the hydrolysis mechanism, two distinct radiolabeled forms of aclidinium were prepared with the radioactive carbon-14 label incorporated into the phenyl or the glycolyl moieties of the molecule (Fig. 1). The phenotyping reaction of aclidinium and its hydrolysis metabolites was performed using human-expressed recombinant P450 isoforms and P450-specific chemical inhibitors and inhibitory antibodies.

2. Materials and methods

2.1. Chemicals

^{14}C-phenyl-AB (^{14}C-phe-AB, 30.2 mCi/mmol) and ^{14}C-glycolyl-AB (^{14}C-glyc-AB, 26.0 mCi/mmol) were synthesized at Quotient BioResearch Ltd. (Northamptonshire, UK). The radiolabeled hydrolysis products ^{14}C-LAS34823 (23.9 mCi/mmol) and ^{14}C-LAS34850 (24.4 mCi/mmol) were prepared by basic hydrolysis from ^{14}C-phe-AB and ^{14}C-glyc-AB, respectively, and further purification (Pharmacokinetics & Drug Metabolism Department, Almirall S.A., Barcelona, Spain). All radiolabeled compounds exhibited purity over 98% (determined by liquid chromatography [LC] with UV and radiometric detection). Stock solutions of 5 mM ^{14}C-phe-AB and 5 mM ^{14}C-glyc-AB were prepared in 0.1N HCl:acetonitrile (10:90, v/v). Stock solutions of 5 mM ^{14}C-LAS34823 and 10 mM ^{14}C-LAS34850 were prepared in aqueous basic solution containing 20% acetonitrile. Non-radiolabeled aclidinium (>99% purity), its alcohol metabolite (LAS34823; [3(R)-hydroxy-1-(3-phenoxy-propyl)-1-azonia-bicyclo[2.2.2]octane, bromide]) and its carboxylic acid metabolite (LAS34850; [dithienyl-glycolic acid, sodium salt]), LAS188638 and LAS101563 standards were synthesized at Ranke Química S.L. (Barcelona, Spain). Working solutions of ^{14}C-phe-AB and ^{14}C-glyc-AB were prepared daily before use in 0.01N HCl:acetonitrile (80:20, v/v) to prevent aclidinium hydrolysis. LC-grade methanol, acetonitrile, dimethylsulphoxide (DMSO), and triethylamine (TEA) were obtained from Scharlab S.L. (Barcelona, Spain). Glucose-6-phosphate, $NADP^+$, glucose-6-phosphate dehydrogenase, 2-thiopheneglyoxylic acid, dithienyl-2-ketone, and Krebs–Henseleit medium with D-glucose were purchased from Sigma–Aldrich (Steinheim, Germany). Williams' E medium and other chemicals used in hepatocyte incubations were purchased from Gibco Invitrogen (Paisley, UK). All other chemicals used were purchased from Sigma–Aldrich (Steinheim, Germany).

2.2. Biological materials

CD-1 mouse (male and female), Sprague–Dawley rat (male and female), New Zealand white rabbit (female), Beagle dog (male), and human (mixed gender, $n = 50$ donors) liver microsomes were purchased from XenoTech (Lenexa, KS, USA). CD-1 mouse (male), Wistar rat (male), New Zealand white rabbit (female) and human (mixed gender, $n = 10$ donors) cryopreserved hepatocytes were purchased from Celsis International (Chicago, USA). Cryopreserved Beagle dog (male) hepatocytes were purchased from XenoTech. Recombinant human P450 (CYP1A1, 1A2, 2C8, 2C9*1, 2C19*1, 2A6, 2B6, 2D6*1, 2E1, 3A4, 3A5, 4A11, 2F2, 4F3A, 4F3B) and flavin-containing monooxigenases (FMO1, FMO3, and FMO5) expressed in microsomes of baculovirus-infected cells (Supersomes™) were

obtained from BD Biosciences (San Jose, CA, USA). All the P450 isoforms contained NADPH-P450 reductase. Selective human P450 antibodies (CYP1A2, 2A6, 2B6, 2C8, 2D6, 2E1, and 3A4/5) were obtained from Gentest (Woburn, MA, USA).

2.3. Liver microsome incubations

All microsomal incubations were carried out in open-to-air polyethylene tubes at 37 °C in a shaking water bath. Microsomal protein (0.5 mg/ml) in 50 mM phosphate buffer (pH 7.4) containing 3 mM $MgCl_2$, 1 mM EDTA, and co-factor generating system (1 mM $NADP^+$, 5 mM glucose-6-phosphate and 2.5 units/ml glucose-6-phosphate dehydrogenase) were placed in a shaking water bath for 3 min at 37 °C. Reactions were initiated by the addition of the test compounds (^{14}C-phe-AB and ^{14}C-glyc-AB incubations) or NADPH-generating system (^{14}C-LAS34823 and ^{14}C-LAS34850 incubations) to give a final incubation volume of 1 ml. Incubations were terminated by the addition of 0.5 ml of ice-cold 0.2N HCl. Aliquots of the incubation samples (0.3 ml) in time-dependent studies were taken at different pre-defined times (15, 30, and 60 min) and terminated by the addition of 0.15 ml of ice-cold 0.2N HCl. Enzyme kinetics studies in human liver microsomes were performed under initial linear conditions with respect to incubation time (15 min for ^{14}C-phe-AB and ^{14}C-glyc-AB and 30 min for ^{14}C-LAS34823 and ^{14}C-LAS34850) and microsomal protein concentration (0.25 mg/ml for ^{14}C-phe-AB and ^{14}C-glyc-AB and 0.5 mg/ml for ^{14}C-LAS34823 and ^{14}C-LAS34850). All incubations were carried out in duplicate, and the concentration of organic solvent (acetonitrile) was kept below 2% (v/v). Parallel incubations were always performed in the incubation buffer as a non-enzymatic hydrolysis evaluation. Sample analysis was conducted using solid phase extraction (SPE)–LC system with radiometric detection.

2.4. Hepatocyte incubations

Immediately before use, hepatocytes were thawed according to the recommended protocol. In brief, frozen cells (approximately 5×10^6 cells/vial) were thawed quickly by gentle shaking in a 37 °C water bath. Immediately after thawing, the hepatocyte suspension was diluted with Williams' E medium (pH 7.4) supplemented with 2.5 μM dexamethasone, 4 μg/ml insulin, 100 units/ml penicillin, 100 μg/ml streptomycin, 2 mM glutamine, and 10% fetal bovine serum pre-warmed to 37 °C. After centrifugation (25 °C, 50 × *g*, 5 min) and medium aspiration, the hepatocyte pellet was resuspended by gentle inversion in 2.0 ml of pre-warmed Krebs–Henseleit buffer (pH 7.4) supplemented with 1 mM $CaCl_2$, 25% $NaHCO_3$, 20 mM HEPES, diluted to 30 ml with the same buffer and washed once. Hepatocyte viability was measured using the trypan blue exclusion method. The initial cell suspension was diluted at 2.1×10^6 viable cells/ml using Krebs–Henseleit buffer (pH 7.4). Incubations were conducted in suspension (2×10^6 viable cells/ml in a total volume of 0.1 ml) for 1 and 2 h in round-bottom glass tubes at 37 °C in an atmosphere of 5% CO_2 and 95% relative humidity (Forma Series II 3121, CO_2 water jacketed incubator, Thermo Scientific, Marietta, OH, USA). Radiolabeled test compounds were incubated at final concentrations of 20 μM. To minimize P450 inhibition, the concentration of organic solvent (acetonitrile) was kept below 1% (v/v). Reactions were terminated by addition of 0.1 ml of ice-cold acetonitrile/1N HCl (90/10, v/v) and incubation samples were immediately frozen at −80 °C until analysis using LC with radiometric detection. All incubations were performed in triplicate and parallel incubations with 75 μM 7-ethoxycoumarin were also performed as a positive control for Phases I and II metabolism.

2.5. Incubations with human recombinant P450 and FMO isoforms

The compounds ^{14}C-Phe-AB (5 μM), ^{14}C-Glyc-AB (5 and 25 μM), and ^{14}C-LAS34823 (5 μM) were incubated in duplicate at 37 °C for 15, 30 and 60 min, respectively, with a panel of recombinant human P450 enzymes (CYP1A1, 1A2, 2B6, 2C8, 2C19, 2D6, 2E1, 3A4, 3A5, 4F2, 4F3A, 4F3B, CYP2A6, 2C9, and 4A11) at 25 pmol of P450/ml and with recombinant FMO1, FMO2, and FMO3 at 0.2 mg of protein/ml. Protein concentration in recombinant human P450 incubations was normalized (0.25 mg/ml) using insect control protein, without esterase and P450 activity. The incubation conditions and sample workup were similar to those described above (Section 2.3).

2.6. Chemical and antibody inhibition studies

Incubations were conducted in human liver microsomes as described above at the following test substance concentrations: 5 μM (^{14}C-LAS34823), 5 and 25 μM (^{14}C-phe-AB and ^{14}C-glyc-AB, respectively) in a final volume of 1 ml. The selective chemical human P450 inhibitors assayed and final concentrations were 1 μM α-naphthoflavone (CYP1A2), 2.5 μM 8-methoxypsolaren (CYP2A6), 10 μM quercetin (CYP2C8), 10 μM sulfaphenazole (CYP2C9), 10 μM omeprazole (CYP2C19), 10 μM quinidine (CYP2D6), 2 μM ketoconazole (CYP3A4), and 2.5 μM 4-methylpyrazole (CYP2E1). After 3 min of pre-incubation at 37 °C, reactions were started by addition of the NADPH generating system (^{14}C-LAS34823) or the test substance (^{14}C-phe-AB and ^{14}C-glyc-AB). After 15 min (^{14}C-phe-AB and^{14}C-glyc-AB) or 30 min (^{14}C-LAS34823), reactions were stopped by the addition of 0.5 ml ice-cold 0.2N HCl. Incubations in the presence of the irreversible CYP2A6 inhibitor 8-methoxypsolaren were preceded by 15 min of pre-incubation time with NADPH before the addition of the test compounds. The final concentration of acetonitrile in the incubation mixtures was 0.7%. To determine the effect of anti-P450 monoclonal antibodies on the metabolism of ^{14}C-LAS34823, ^{14}C-phe-AB, and ^{14}C-glyc-AB, incubations were conducted in the presence of 5 μl antibody/100 mg microsomal protein in all cases except for CYP3A4 antibody (10 μl/100 mg). The different monoclonal human P450 antibodies were added to human liver microsomes (0.5 ml) and incubated for 20 min on ice. Incubations were conducted as described above in a final volume of 1 ml. The final concentration of acetonitrile in the incubation mixtures was 0.2%. All incubations were carried out in duplicate. Sample analysis was conducted using SPE–LC system with radiometric detection.

2.7. LC analysis with radiometric detection

2.7.1. Method A

Microsomal incubation samples were centrifuged for 10 min (4 °C) at 2000 × *g* (Heraeus Omnifuge 2.0RS, Heraeus Sepatech GmbH, Osterode, Germany), and the supernatant (1.5 ml) was analyzed by on-line SPE (Prospekt, Spark-Holland, Emmen, Netherlands) coupled to LC (Waters Alliance 2695 system, Milford, MA, USA) with radiometric flow scintillation detection (Packard 150TR, PerkinElmer, Downers Grove, IL, USA), and UV detection at 220 and 240 nm (Waters 2996 Photo Diode Array). Briefly, following activation of an SPE Waters Oasis HLB cartridge (10 × 2 mm, 30 μm, 15 mg) with 1 ml of methanol and conditioning with 1 ml of pure water, incubation samples (1.5 ml) were passed through the cartridges and cleaned up with 0.5 ml of 40 mM formic acid. The compounds retained were eluted directly into the LC column using the mobile phase for 20 min. Chromatographic separation was achieved using a Symmetry C_{18} column (250 × 4.6 mm; 5 μm; Waters), eluted at a constant flow rate of 1 ml/min. The mobile phase consisted of (A) 40 mM

ammonium formate containing 0.1% triethylamine (pH 4.5) and (B) acetonitrile as solvents. Samples were separated using a linear gradient from 10% to 55% B within 30 min. The mobile phase was returned to the starting solvent mixture in 1 min and the system equilibrated for 8 min between runs. Incubation samples during LC analysis were always kept at 4 °C in order to prevent aclidinium ester cleavage. Chromatographic data were processed using Millenium[32] software, version 3.2 (Waters). The analytical method was validated for selectivity, linearity, quantitation limit, intra- and inter-batch precision and accuracy, recovery, and stability, demonstrating the suitability of this method for the quantitative measurements of test compounds and their respective metabolites.

2.7.2. Method B

Hepatocyte incubation samples were centrifuged for 10 min (4 °C) at 2000 × *g* and the supernatant was analyzed by LC with radiometric detection. Chromatographic separation was achieved using a Luna Phenyl-Hexyl column (250 × 4.6 mm; 5 μm; Phenomenex, Torrance, CA, USA) and eluted at a constant flow rate of 0.8 ml/min. The mobile phase consisted of mixtures of (A) 1 M ammonium acetate:water:acetonitrile (10:890:100, v/v/v) and (B) 1 M ammonium acetate:water:acetonitrile (10:290:700, v/v/v). An initial proportion of 10% B was maintained for 1 min after sample injection (75 μl), followed by a linear gradient from 10% to 90% B within 7 min. B was maintained at 90% for 12 min and the mobile phase was returned to the starting solvent mixture in 1 min. The system was equilibrated for 7 min between runs. All LC analysis samples were also kept at +4 °C in order to prevent aclidinium ester cleavage. Chromatographic data were processed as described above.

The designation of the individual metabolites was coded to specify the structure and the origin of the biotransformation product. Thus, the initial letter refers to the parent compound origin: "M" metabolites formed from ^{14}C-phe-AB and ^{14}C-LAS34823 incubations, and "m" metabolites formed from ^{14}C-glyc-AB and ^{14}C-LAS34850 incubations. The number given to a metabolite corresponds to a specific chemical entity identified according to the observed chromatographic retention time in the radiochromatograms. For example, metabolites M4 and m5 correspond to the same biotransformation product obtained in ^{14}C-phe-AB or in ^{14}C-glyc-AB incubations, respectively. Other minor LAS34823, LAS34850, and aclidinium metabolites were coded as M/m, followed by a lower-case subscript letter (e.g.: M_f). The identification of metabolites was based on comparison with standards and LC–MS/MS analysis.

2.8. LC–MS and LC–MS/MS analysis

The LC–MS system used for analysis of incubation supernatants consisted of an Agilent 1100 LC separation module (Waldbronn, Germany) coupled to an API Sciex 3000 triple quadrupole mass spectrometer (PerkinElmer, Boston, MA, USA). Chromatographic separation was achieved using a Symmetry C_{18} column (100 × 2.6 mm; 3.5 μm; Waters) with elution at a constant flow rate of 0.5 ml/min. The mobile phase consisted of (A) 10 mM ammonium formate at pH 4.5 and (B) acetonitrile as solvents. An initial proportion of 100% A was maintained for 2 min after sample injection, followed by a linear gradient from 0% to 45% B within 28 min. The mobile phase was returned to the starting solvent mixture in 1 min, and the system was equilibrated for 7 min between runs. Mass spectrometry was conducted with electrospray ion source operating in positive ion mode (AB, LAS34823 and their metabolites) or negative ion mode (AB, LAS34850 and their metabolites). The ion spray interface temperature was set at 450 °C (positive mode) and at 250 °C (negative mode) using nitrogen as a nebulizing gas. LC/MS and LC/MS/MS experiments were performed at a voltage between 2.0 and 4.5 kV (positive mode) and 1.5 kV (negative mode). The collision energy was between 30–45 eV in positive mode and 5–30 eV in negative mode.

Metabolite identification was established by comparison with synthetic standards, when available, using retention time and mass spectral data.

2.9. NMR analysis

M1 (approximately 50 μg) isolated from an incubation of non-radiolabeled LAS34823 with rat and rabbit liver microsomes in the presence of NADPH was characterized using ^{1}H nuclear magnetic resonance (NMR). The ^{1}H NMR spectrum was recorded in a Varian Mercury-plus NMR spectrometer (Palo Alto, CA, USA) at 400 MHz. The sample was dissolved in deuterated DMSO-d_6. Chemical shifts were reported in the δ scale (ppm) by using DMSO-d_6 signal at 2.49 ppm as a reference.

2.10. Statistics and data analysis

Data from kinetic studies were analyzed by non-linear regression analysis with Grafit 5.0 (Erithacus Software, Staines, UK) using models for Michaelis–Menten kinetics, biphasic kinetics, or sigmoidal kinetics. In those cases where non-enzymatic hydrolysis occurred, the determination of the apparent Michaelis–Menten parameters (K_m and V_{max}) and non-enzymatic hydrolysis rate constant (K_h) were carried out using the following equation [4]:

$$\upsilon = \frac{V_{max}[S]}{K_m + [S]} + K_h[S]$$

where υ is the formation rate, [*S*] is the substrate concentration, K_m is the apparent Michaelis–Menten constant, V_{max} is the apparent maximum velocity, and K_h is the non-enzymatic hydrolysis rate constant. The goodness-of-fit criteria used to select the model comprised visual inspection, consideration of the randomness of residuals, and the standard error of the parameters.

3. Results

3.1. Validation of the LC method with radiometric detection

The oxidative and NADPH-dependent metabolites of ^{14}C-phe-AB and ^{14}C-glyc-AB were formed at a very low extent. Therefore, on-line SPE was necessary to improve the sensitivity of the radiometric detection method. To ensure the applicability of this method for the analysis of incubation samples, the method was fully validated for accuracy, precision, linearity, limit of quantitation, and compound stability. Overall, the analytical method demonstrated its suitability for the quantitative measurement of AB metabolites originated in vitro. The extraction recovery for test compounds and oxidative and hydrolysis metabolites ranged from 80% to 108%. For each day of incubation, calibration standards ($n = 5$, $r > 0.995$) and quality-control samples ($n = 2$ at three different concentrations) of the corresponding radiolabeled test compounds were prepared in incubation buffer and treated as incubation samples. Intra- and inter-batch precision and accuracy of measurements of quality-control samples, expressed as coefficient of variation, were always lower than 10% at all concentration levels. Following incubations of ^{14}C-phe-AB, ^{14}C-glyc-AB, ^{14}C-LAS34823, and ^{14}C-LAS34850 in human liver microsomes in the presence of NADPH, the supernatant recoveries based on total radioactivity peak area (sum of peak areas of all metabolites and

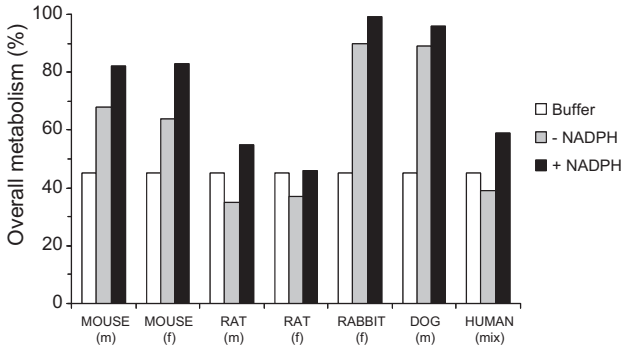

Fig. 2. Percentage of metabolism of ^{14}C-phe-AB (50 μM) after 60 min in incubation buffer and in liver microsomes of different species (m): male; (f): female; (mix): mixed gender. Each bar represents the mean of duplicate determinations (<15% variance).

remaining parent compound) were, in all cases, greater than 85% with respect the radioactivity peak area of the test compound in control incubations. All test compounds were shown to be stable during the sample analysis.

3.2. Metabolism of aclidinium bromide in liver microsomes

Incubations of ^{14}C-phe-AB and ^{14}C-glyc-AB in liver microsomes (0.5 mg protein/ml) of animal species and humans were conducted at a concentration of 50 μM in order to detect minor metabolites formed during incubations. Both radiolabeled forms of AB were incubated for 60 min in order to evaluate differences in their metabolism. Aclidinium was shown to be an unstable ester in the incubation buffer (pH 7.4). A species comparison of the overall metabolism of ^{14}C-phe-AB after 60 min of incubation is represented in Fig. 2. The hydrolysis half-life in the assay buffer (pH 7.4, 37 °C) was around 70 min. The in vitro disappearance half-life of ^{14}C-phe-AB in the absence of NADPH followed the rank order rat (male, female), 100 min ≈ human, 93 min > mouse (male), 42 min ≈ mouse (female), 37 min > dog 19 min ≈ rabbit, 16 min. The results obtained following incubation of ^{14}C-glyc-AB were similar to those obtained with ^{14}C-phe-AB. Possible metabolites other than the hydrolysis metabolites (LAS34823 and LAS34850) were not observed in incubations without NADPH, suggesting that the oxidative metabolism of AB in liver microsomes is primarily mediated by P450.

According to these results, enzymatic hydrolysis of aclidinium in human and rat liver microsomes was not observed, suggesting that the potential presence of esterases responsible for AB hydrolysis in the microsomal fractions of these two species has little relevance. To confirm this, additional incubations of ^{14}C-phe-AB (5 μM) in human liver microsomes (1 and 2 mg/ml) were investigated in the absence of NADPH and incubation buffer. There were slight differences in the formation of the hydrolysis metabolites between human liver microsomes and the incubation buffer. In fact, the net enzymatic hydrolysis of AB at 2 mg/ml was less than 20% after 60 min of incubation. These results are in agreement with previous studies where BChE content was demonstrated to be low in human liver microsomes and consequently, the enzymatic hydrolysis of AB had little scientific relevance compared to non-enzymatic hydrolysis [4].

Additional oxidative metabolism of aclidinium was observed in the presence of NADPH. In this case, the in vitro disappearance half-life value for the overall metabolism of ^{14}C-phe-AB followed the rank order rat (female), 73 min > rat (male), 56 min ≈ human, 52 min > mouse (male, female), 23 min > dog 13 min ≈ rabbit, 8 min. Similar values were also obtained for ^{14}C-glyc-AB.

The radioactive metabolite profiles of liver microsomal incubations of ^{14}C-phe-AB and ^{14}C-glyc-AB (50 μM) with NADPH were qualitatively similar across species and representative chromatograms are shown in Fig. 3. After incubation of ^{14}C-phe-AB, the major metabolite observed in all species was M2 (LAS34823, alcohol metabolite), whilst other minor and NADPH-dependent metabolites M1, M3, M4, M5, and M6 were also observed in different species. In the same way, the acid metabolite m3 (LAS34850) and metabolite m2 were the main metabolites in ^{14}C-glyc-AB incubations. In addition, trace amounts of other metabolites (m1, m_a, m4, and m5) were also observed in some species.

Incubation of ^{14}C-LAS34823 with pooled human liver microsomes revealed the NADPH-dependent metabolism of this compound to metabolite M1 (Fig. 3). Traces of other hydroxylated LAS34823 metabolites were also observed using MS/MS detection (Section 3.4.14).

After incubation of ^{14}C-LAS34850 in incubation buffer, a radioactive peak was observed with a retention time of 31.5 min. The formation of this compound was independent of the incubation time. According to its chromatographic retention time and comparison of the MS spectra with a commercial standard, this artifact was identified as the compound di-2-thienyl ketone (see below). In the presence of NADPH-generating system, the artifact disappeared and a new radioactive peak (t_{ret} 19 min) named m_a was detected (Fig. 3). The formation of m_a was very rapid and did not increase with incubation time. Further investigations at different microsomal protein concentrations (0.25, 0.5, and 1 mg/ml) demonstrated that m_a formation was non-enzymatic and dependent only on NADPH. This point was confirmed by performing additional incubations where the presence of $NADP^+$ (oxidized form) in buffer solution failed to generate m_a (results not shown). The chemical structure of m_a was tentatively elucidated by LC–MS/MS as the compound 2-dithienylacetic acid (see below). The presence of an acidic moiety in the chemical structure of m_a was also confirmed by the chromatographic behaviour of this compound, increasing its retention time with decreasing pH of the mobile phase in the same way observed for LAS34850. No other radioactive peaks were observed in the chromatograms, which suggests that enzymatic metabolism of LAS34850 does not occur.

The metabolites found in liver microsomal incubations of ^{14}C-phe-AB and ^{14}C-glyc-AB are summarized in Tables 1 and 2, respectively.

3.3. Metabolism of aclidinium bromide in hepatocytes

The stability of AB in Krebs–Henseleit incubation medium (pH 7.4) showed an apparent elimination half-life ($t_{1/2}$) of 56 min, indicative of considerable non-enzymatic hydrolysis in the incubation conditions. The percentages of metabolism for ^{14}C-phe-AB and ^{14}C-glyc-AB were high in all species evaluated after 2 h of incubation, ranging from 60% (human) to almost 100% (rabbit).

The major radioactive metabolites of ^{14}C-phe-AB (20 μM) in all species were M2 (LAS34823) and M1 (LAS188638). Representative chromatograms obtained in rabbit and human hepatocytes are shown in Fig. 4. Rabbit hepatocytes showed the highest rate of M1 formation (around 50%) and intermediate values (between 9% and 16%) were observed for mouse, rat and human hepatocytes. In contrast, dog hepatocytes showed the lowest formation of M1 (Table 1). Also, two polar radioactive metabolites were observed in mouse, rat, and rabbit hepatocytes. Their structures were identified by LC–MS/MS as the glucuronide conjugates of M1 and M2, i.e., $M1_{gluc}$ and $M2_{gluc}$, respectively (see below). Rabbit hepatocytes produced the highest amount of glucuronide conjugates. Although M1 and M2 were generated to a similar

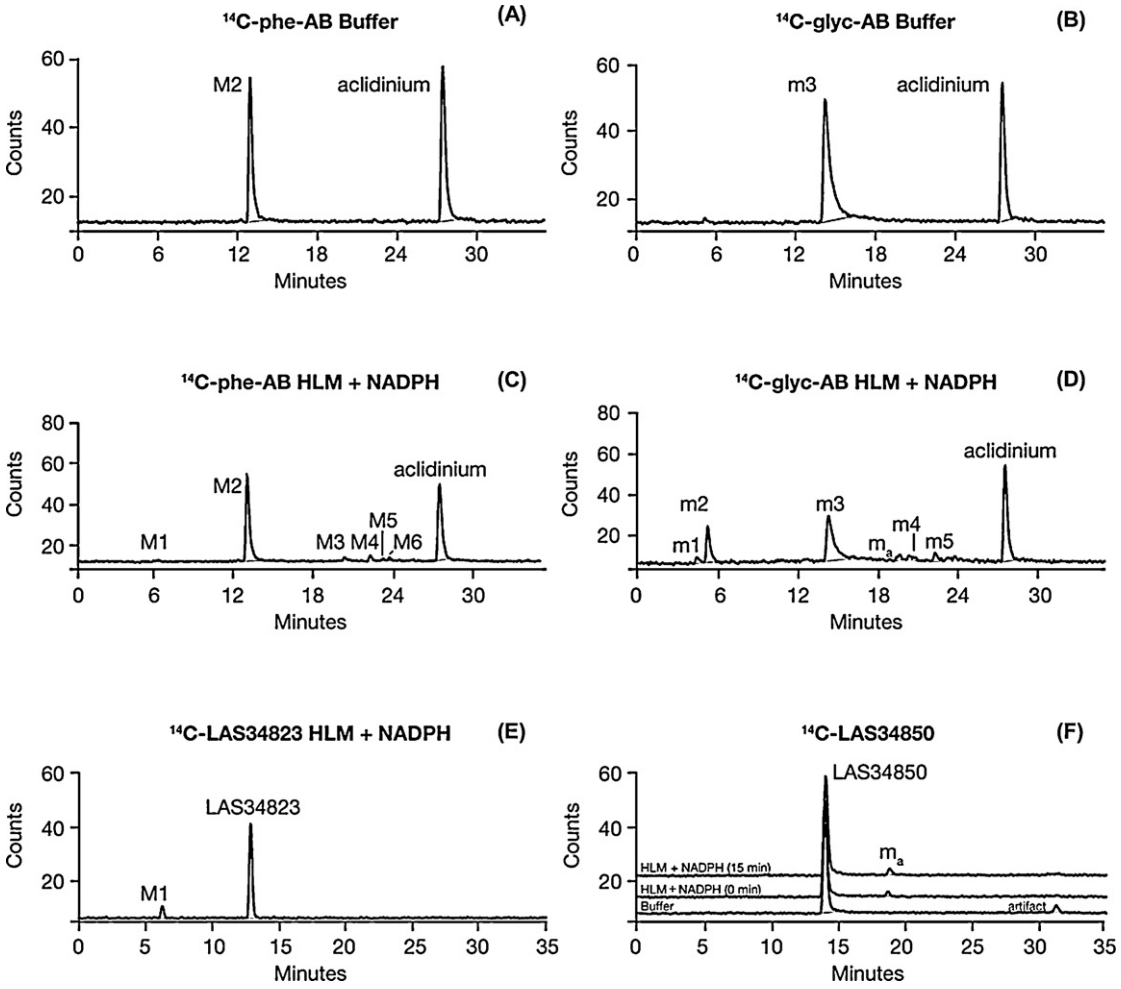

Fig. 3. Representative chromatograms (Method A) showing metabolite profiles of 50 μM ^{14}C-phe-AB and ^{14}C-glyc-AB in phosphate buffer (A, B), 50 μM ^{14}C-phe-AB and ^{14}C-glyc-AB in human liver microsomes (HLM) with NADPH (C, D), 10 μM ^{14}C-LAS34823 in human liver microsomes with NADPH (E), and 10 μM ^{14}C-LAS34850 in phosphate buffer and human liver microsomes with/without NADPH (F).

extent in incubations, $M2_{gluc}$ was formed at much lower levels than $M1_{gluc}$. Thus, it is reasonable to propose that M1 glucuronidation occurs at the hydroxyl moiety located at the para position of the phenyl ring.

The major radioactive metabolite of ^{14}C-glyc-AB (20 μM) in all species was m3 (LAS34850), which accounted for 85%, 51%, 100%, 72%, and 64% in mouse, rat, rabbit, dog, and human hepatocytes, respectively. Two minor polar metabolites were also observed in

Table 1
Metabolites of ^{14}C-phe-aclidinium bromide detected in liver microsomes and hepatocytes. ^{14}C-phe-AB was incubated with liver microsomes (0.5 mg/ml and NADPH-generating system) and hepatocytes (2 M cells/ml) for 60 and 120 min, respectively. Results expressed as percentage of total peak area of the radiochromatograms.

Metabolite	RT	Mouse (m)	Mouse (f)	Rat (m)	Rat (f)	Rabbit (f)	Dog (m)	Human (mix)
Liver microsomes								
M1	6.2 (8.8)	3.7	3.5	7.1	4.3	8.2	9.3	0.9
M2	12.6 (13.2)	75.7	75.4	36.5	36.5	91.0	85.7	47.5
M3	19.9 (20.2)	d	ND	ND	ND	d	ND	2.1
M4	21.8 (22.4)	1.1	1.3	2.0	1.1	d	0.9	2.5
M5	22.6 (25.3)	d	1.3	1.4	ND	ND	ND	0.7
M6	23.1 (25.4)	0.9	1.0	2.0	ND	d	ND	1.1
Hepatocytes								
M1gluc	3.9B (3.9)	2.7	–	2.5	–	14.8	ND	ND
M2gluc	4.4B (4.4)	0.5	–	0.6	–	1.4	ND	ND
M1	8.7B (8.8)	15.9	–	13.9	–	51.2	1.7	9.2
M2	12.2B (13.2)	73.1	–	59.5	–	32.6	87.3	76.2

Mean values from duplicate (liver microsomes) and triplicate (hepatocytes) experiments.
m, male; f, female; mix, mixed gender.
RT, retention time (minutes) using method A, if not otherwise indicated. In brackets, retention times using LC–MS/MS.
–: assay not performed.
ND, not detected, below 0.5% of total radioactive peak area.
d, metabolite detected at shorter incubation times.
Metabolites generated from ^{14}C-phe-AB incubations were coded as "M". Metabolites M1gluc and M2gluc were not observed in microsomal incubation, whereas M3, M4, M5, and M6 were not observed in hepatocyte incubations.

Table 2
Metabolites of ^{14}C-glyc-aclidinium bromide detected in liver microsomes and hepatocytes. ^{14}C-glyc-AB was incubated with liver microsomes (0.5 mg/ml and NADPH-generating system) and hepatocytes (2 M cells/ml) for 60 and 120 min, respectively. Results expressed as percentage of total peak area of the radiochromatograms.

Metabolite	RT	Mouse (m)	Mouse (f)	Rat (m)	Rat (f)	Rabbit (f)	Dog (m)	Human (mix)
Liver microsomes								
m1	4.4 (1.5)	3.1	2.3	ND	ND	1.8	ND	2.5
m2	5.1 (3.0)	23.5	29.9	15.5	9.6	19.5	16.3	13.7
m3	14.2 (16.6)	57.2	52.6	33.1	36.0	74.1	76.1	33.7
m_a	19.3 (18.6)	3.4	3.0	2.8	2.0	4.6	4.9	2.8
m4 (M3)	19.9 (20.2)	d	ND	d	ND	d	ND	3.1
m5 (M4)	21.8 (22.4)	1.2	1.3	1.7	0.9	d	1.4	3.3
m6 (M5)	22.6 (25.3)	ND	1.0	1.0	ND	ND	ND	ND
m7 (M6)	23.1 (25.4)	ND	0.9	ND	1.5	ND	ND	ND
Hepatocytes								
m_x	3.5B (ND)	0.5	–	0.9	–	ND	0.8	ND
m1	ND	ND	–	ND	–	ND	ND	ND
m2	3.9B (3.0)	1.4	–	6.7	–	ND	0.8	ND
m3	8.1B (16.6)	85.4	–	50.6	–	100	71.8	63.7
m_a	ND	ND	–	ND	–	ND	ND	ND

Mean values from duplicate (liver microsomes) and triplicate (hepatocytes) experiments.
m, male; f, female; mix, mixed gender.
RT, retention time (minutes) using method A, if not otherwise indicated. In brackets, retention times using LC–MS/MS.
–: assay not performed.
ND, not detected, below 0.5% of total radioactive peak area.
d, metabolite detected at shorter incubation times.
Metabolites generated from ^{14}C-glyc-AB incubations were coded as "m". Metabolite m_x, was not observed in microsomal incubation, whereas m4, m5, m6, and m7 were not observed in hepatocyte incubations.

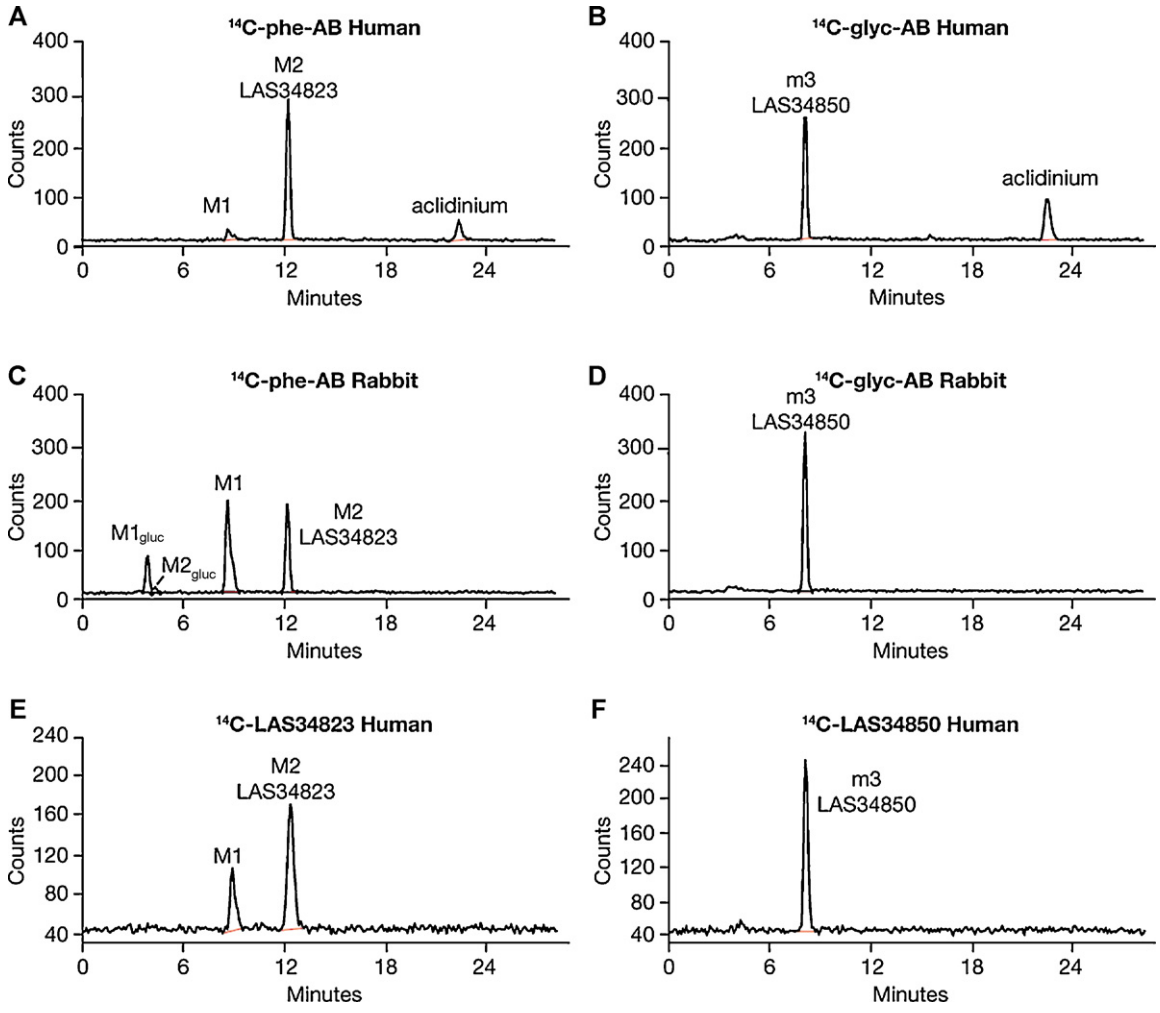

Fig. 4. Representative chromatograms (Method B) showing metabolite profiles of ^{14}C-phe-AB and ^{14}C-glyc-AB in human hepatocytes (A, B), ^{14}C-phe-AB and ^{14}C-glyc-AB in rabbit hepatocytes (C, D), ^{14}C-LAS34823 and ^{14}C-LAS34850 in human hepatocytes (E, F). Test substances were incubated at a final concentration of 20 μM.

mouse, rat, and dog cryopreserved hepatocytes. One of these minor metabolites was identified as 2-thiopheneglyoxylic acid (m2), accounting for 1–7% of total radioactivity. Metabolite m_x was only observed in mouse, rat, and dog hepatocytes at a very low concentration (Table 2).

Metabolite m2 was only observed in ^{14}C-glyc-AB incubations and not in ^{14}C-phe-AB incubations (Table 2, Fig. 3), which supports the hypothesis that the metabolic attack took place at the thiopheneglyoxylic moiety of the molecule. Nevertheless, this metabolite was not observed following incubation of ^{14}C-LAS34850, suggesting that m2 might originate from the parent compound only.

Following incubation of ^{14}C-LAS34823 (20 μM) with human hepatocytes, only M1 (LAS188638) was observed, accounting for 28% of the radioactivity after an incubation time of 2 h. The acid metabolite ^{14}C-LAS34850 (20 μM) was not metabolized by human hepatocytes during the 2 h of incubation (Fig. 4).

3.4. Metabolite identification

The identification of metabolites was based on comparison with standards (when available) using LC-ESI-MS/MS in either positive or negative mode depending on the compound or metabolite of

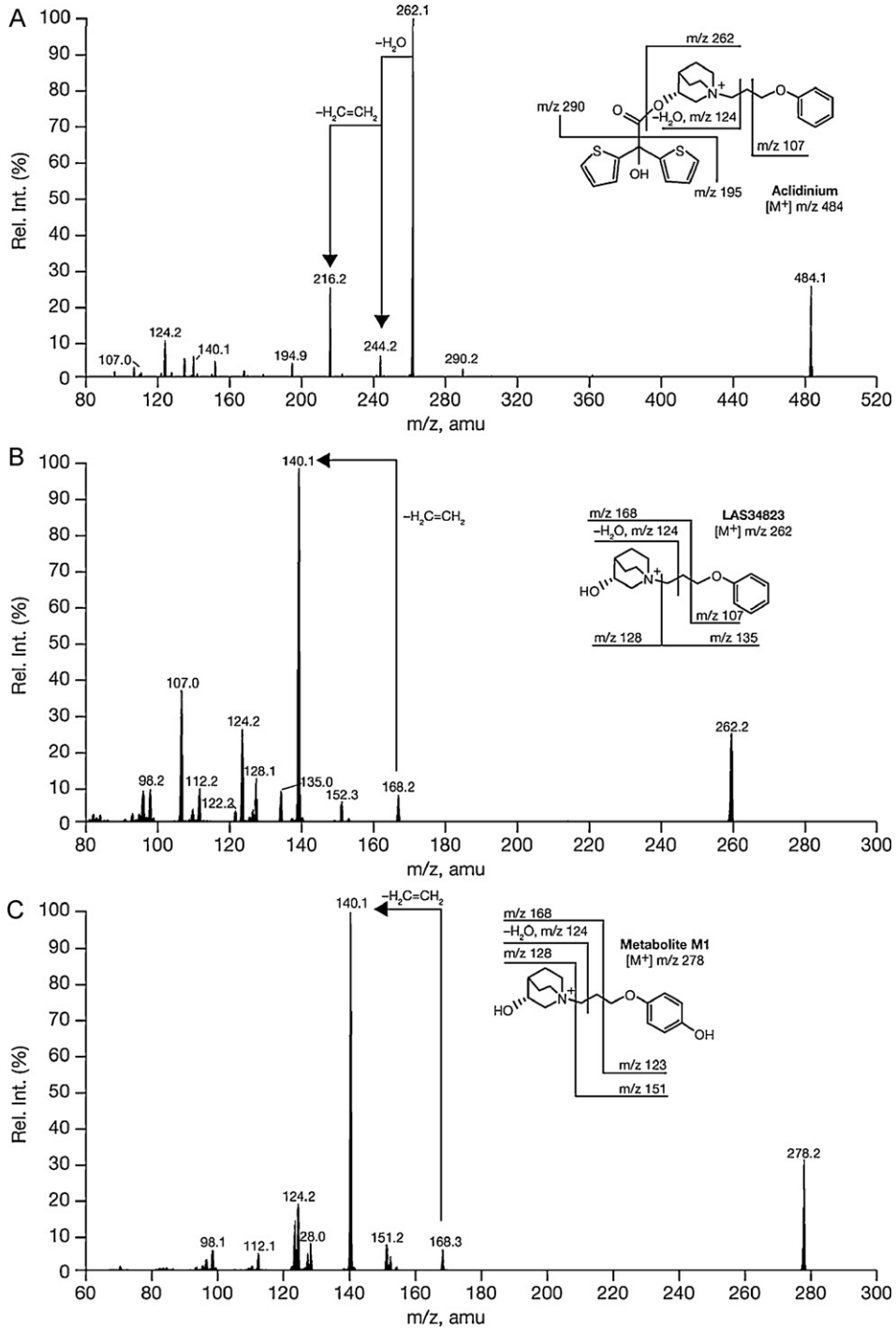

Fig. 5. MS/MS spectra of (A) aclidinium bromide, (B) metabolite M2 (LAS34823), and (C) metabolite M1 (LAS188638).

interest. The exact position of hydrolylation on the terminal phenyl ring of M1 was conducted using ^{1}H NMR.

3.4.1. Aclidinium bromide

The MS/MS spectrum of aclidinium in positive mode gave a major fragment ion at *m/z* 262, corresponding to the molecular ion of the alcohol derivative LAS34823. This fragment ion *m/z* 262 led to the sequential loss of H_2O (*m/z* 244) and $H_2C{=}CH_2$ (*m/z* 216) as shown in Fig. 5A. This fragmentation pattern is in accordance with the MS/MS fragmentation of different N-alkyl derivatives of 3-quinuclidinol molecules described by Bednár et al. [7].

3.4.2. Metabolite M2 (LAS34823)

LC–MS analysis of LAS34823 using ESI in positive mode showed a molecular ion [M$^+$] of *m/z* 262. The product ion spectrum showed a fragment ion of *m/z* 140 as the most abundant. The fragment ions observed at *m/z* 168 and 107 suggest the loss of the phenoxymethyl moiety. The fragment of *m/z* 135 points to the loss of the phenoxypropyl moiety (Fig. 5B).

3.4.3. Metabolite M1 (LAS188638)

This metabolite presented a molecular ion [M$^+$] at *m/z* 278. The fragments obtained at *m/z* 168, 140, and 124 were also observed in the spectrum of M2 (LAS34823), which suggests that the 3-quinuclidinol moiety remains unchanged. The observed fragments at *m/z* 123 (107 + 16 amu) and 151 (135 + 16 amu) clearly suggest hydroxylation at the phenyl ring (Fig. 5C). In order to determine the exact position of hydroxylation, this metabolite was isolated and purified from rat and rabbit liver microsomal incubations for further analysis by ^{1}H NMR. The integrals of the aromatic region revealed that the point of hydroxylation was at the 4-position, since the spectrum showed two doublets (at a proportion 1:1) with a coupling constant of J = 8 Hz. This was later confirmed with the synthesis of the authentic standard. The LC–MS/MS analysis showed the same chromatographic retention time and mass fragmentation for both M1 and the authentic standard (LAS188638).

3.4.4. Metabolites $M1_{gluc}$ and $M2_{gluc}$

The formation of these conjugated metabolites was observed in hepatocyte incubations of ^{14}C-Phe-AB, and their identification was conducted using the LC–MS/MS in multiple reaction monitoring (MRM) mode. The theoretical transitions corresponding to the loss of the glucuronic acid moiety (176 Da) of the potential glucuronides of M1 and M2 (*m/z* 454 > 278 and *m/z* 438 > 262, respectively) were monitored. The radioactive peak with a retention time of 4.4 min showed a peak at the MRM transition of *m/z* 454 > 278, which corresponds to a glucuronide of M1. Similarly, the radioactive peak observed at 5.1 min presented a peak at the transition *m/z* 438 > 262, which strongly suggests the formation of a glucuronide derivative of metabolite M2. Additional incubations of rabbit and mouse hepatocyte samples with β-glucuronidase from Helix Pomatia demonstrated a decrease in the radioactive peak areas, although both glucuronide metabolites were highly resistant to enzymatic hydrolysis (results not shown).

3.4.5. Metabolite m3 (LAS34850)

This compound presented two major peaks at *m/z* 239 and *m/z* 195 in negative ESI mode (Table 3). The fragment of *m/z* 239 corresponds to the molecular ion [M − H]$^-$, whereas the fragment *m/z* 195 may be assigned to decarboxylation (in source collision-induced dissociation) of the molecular ion [8]. Additionally, a minor ion at *m/z* 285 was consistent with the formation of an adduct with the formate present in the mobile phase [M + HCOO]$^-$, a common process described in the literature [9,10]. The product ion mass spectrum of *m/z* 239 gave only the fragment of *m/z* 195, suggesting the loss of CO_2 from the carboxylic acid group. The mass fragmentation of the product ion of *m/z* 195 gave a main fragment ion at *m/z* 83, which is in accordance with the loss of a thiophene ring.

3.4.6. Metabolite m1 (LAS101563)

MS/MS (negative mode) characterization showed the molecular ion at *m/z* 157 and a peak at *m/z* 113 (Table 3). Moreover, a formate adduct was also observed in the MS spectrum (157 + 46), confirming the presence of a carboxylic acid moiety in its structure, as observed for LAS34850 and m2. The chromatographic retention time and the mass fragmentation were identical to those of the authentic standard LAS101563 (hydroxyl-2-thienylacetic acid).

3.4.7. Metabolite m2 (2-thiopheneglyoxylic acid)

The MS (negative mode) spectrum showed a molecular ion at *m/z* 155. The peak observed at *m/z* 201 would be also compatible with the formation of an adduct with formic acid (Table 3). Further MS/MS characterization gave a single fragment at *m/z* 83, corresponding to the thiophene ring. The LC-MS analysis showed the same chromatographic retention time and mass fragmentation of the authentic standard 2-thiopheneglyoxylic acid.

3.4.8. Metabolite m_a (LAS101565)

The full scan spectrum (negative mode) presented peaks at *m/z* 269, *m/z* 223, and *m/z* 179 (Table 3). The peak of *m/z* 223

Table 3
MS and MS/MS spectral data of ^{14}C-glyc-AB metabolites.

Metabolite	MS spectra		MS/MS spectra
	m/z	Tentative assignation	Relevant product ions (*m/z*)
m3	285 (15)	[M + HCOO]$^-$	239 (100); 195 (35)
(LAS34850)	239 (91)	[M − H]$^-$	239 (20); 195 (100)
	195 (100)	[M − H − CO_2]$^-$	195 (100); 83 (10)
	137 (5)	na	–
m1	203 (20)	[M + HCOO]$^-$	–
(LAS101563)	157 (100)	[M − H]$^-$	157 (15); 113 (100)
	113 (20)	[M − H − CO_2]$^-$	–
m2	201 (5)	[M + HCOO]$^-$	201 (50); 155 (100)
(2-thiopheneglyoxylic acid)	155 (100)	[M − H]$^-$	155 (15); 83 (100)
	89 (7)	na	–
	83 (55)	[C_4H_3S]$^-$	–
m_a	269 (77)	[M + HCOO]$^-$	269 (75); 223 (63); 179 (100)
(LAS101565)	223 (61)	[M − H]$^-$	223 (100); 179 (100)
	179 (100)	[M − H − CO_2]$^-$	178/179 (75/50); 146/147 (75/50); 133 (92); 107 (80); 83 (100)

Data in parenthesis: relative abundance (%) in the spectrum.
na: not assigned.
–: MS/MS spectrum not performed.

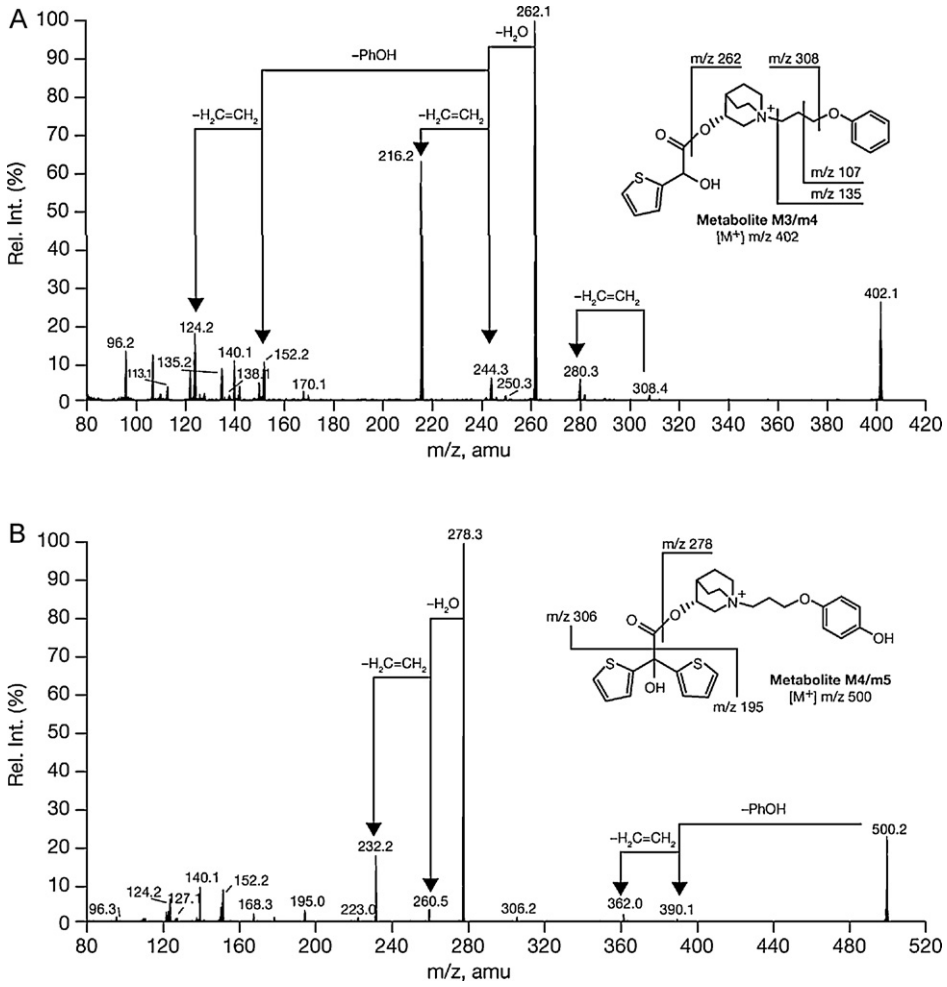

Fig. 6. MS/MS spectra of (A) M3/m4 and (B) M4/m5 metabolites.

corresponds to the molecular ion $[M - H]^-$. The peak observed at *m*/*z* 269 is compatible with the formation of a formate adduct, which was confirmed by further MS/MS analysis. The fragment of *m*/*z* 195 may be assigned to the decarboxylation of the molecular ion, in analogy to LAS34850 and other acidic metabolites. Product ion spectrum of *m*/*z* 179 showed abundant ions at *m*/*z* 178, 146, 133, 107, and 83. The LC–MS analysis showed the same chromatographic retention time of the authentic standard LAS101565.

3.4.9. LAS34850 artifact

In incubations of ^{14}C-LAS34850 in phosphate buffer, a radioactive chromatographic peak appeared at a retention time of 31.4 min (Fig. 3), which was associated with a degradation product or artifact of LAS34850. The commercially available compound dithienyl-2-ketone presented the same retention time and identical UV spectrum with a λ_{max} at 315 nm. Further analysis using the LC–MS method confirmed identical retention times (26.6 min) and identical mass fragmentation pattern in positive ESI mode (molecular ion at *m*/*z* 195). Product ion scans of *m*/*z* 195 showed a fragment at *m*/*z* 111, corresponding to the loss of one thiophene ring. This compound was not ionizable in negative ESI mode.

3.4.10. Metabolite M3/m4

The MS/MS (positive mode) of the molecular ion of *m*/*z* 402 presented major fragments at *m*/*z* 262 and 216, corresponding to the intact quinuclidinol portion of the molecule. These intact fragments indicate that the biotransformation occurs at the thiopheneglyoxylic acid moiety of the molecule. The product ion spectrum showed fragments at *m*/*z* 308 and *m*/*z* 280, which suggests that a thiophene ring has been removed from the structure, corresponding to a net loss of 82 Da (Fig. 6A).

3.4.11. Metabolite M4/m5

This metabolite presented an ion mass spectrum of *m*/*z* 500, which is 16 Da higher than that of the parent compound. The most prominent fragment (*m*/*z* 278) pointed to a hydroxylation occurring at the quinuclidinol portion of the molecule. The presence of the minor fragments of *m*/*z* 140, 362, and 390 suggested that the hydroxylation took place at the phenyl ring in a manner similar to that observed in the formation of M1 (Fig. 6B). To confirm this hypothesis, an M4-purified sample obtained from incubations in liver microsomes was subjected to basic hydrolysis in order to generate the alcohol derivative of this metabolite, which matched the retention time and MS/MS spectrum of M1.

3.4.12. Metabolites M5/m6 and M6/m7

Metabolites M5/m6 and M6/m7 were obtained in very low quantities and the chromatographic resolution was poor. These two metabolites presented a molecular ion of *m*/*z* 500 which is consistent with oxidation of the parent compound. In both cases, the MS/MS spectra showed a fragment of *m*/*z* 262, which is characteristic of an intact quinuclidinol moiety. In addition, a fragment of *m*/*z* 401 clearly points out to an oxidation at one of the thiophene rings. Nonetheless, the MS/MS spectra did not provide

sufficient information to distinguish between C-oxidation (hydroxylation) and S-oxidation.

3.4.13. Metabolite m_x

This polar compound was present as a minor metabolite in incubations of ^{14}C-glyc-AB in mouse, rat, and dog hepatocytes, although the low amounts prevented its characterization by LC–MS/MS.

3.4.14. Other minor metabolites

Additionally, other minor metabolites were detected by LC–MS but were below the level of radiometric detection. Four minor metabolites (M_a, M_b, M_c, and M_d) with a molecular ion at *m/z* 278 were observed in AB and LAS34823 incubations. The MS spectra of two of them (M_a and M_b) confirmed the hydroxylation on the phenyl ring of LAS34823, hence constituting a positional isomer of M1. M_c presented a mass fragmentation pattern different from M1, with a clear loss of water and the appearance of an ion at *m/z* 156 (140 + 16) as the major fragment ion, suggesting that hydroxylation would take place at the 3-quinuclidinol group. Supporting this hypothesis, the fragments at *m/z* 107 and 135 remained unchanged. M_d characterization was not possible due to its low concentration. Metabolite M_e presented a molecular ion *m/z* 408 and a major fragment of 186 Da, which is 76 Da less than the major fragment (*m/z* 262) of LAS34823, consistent with the loss of the phenyl ring. Another metabolite presented a molecular ion of *m/z* 400 (M_f, t_{ret} 23.8 min). This molecular ion and the fragments at *m/z* 152, 135, 124, and 107 suggested that the quinuclidinol portion of the molecule remained intact. This fact implies that the biotransformation should take place at one of the thiophene rings, in a similar way already observed for M3/m4, with the final loss of a thiophene ring. The presence of a fragment of *m/z* 111 strongly suggests oxidation of the alcohol moiety of M3/m4 to a ketone derivative. In addition, other minor glucuronide metabolites in rat and mouse hepatocytes were also observed in LC–MS/MS (MRM mode) analysis using the transition *m/z* 454 > 278, consistent with structural isomers of $M1_{gluc}$.

3.5. Enzyme kinetics

The enzyme kinetics of ^{14}C-LAS34823, ^{14}C-LAS34850, ^{14}C-phe-AB, and ^{14}C-glyc-AB metabolism in human liver microsomes was determined. The metabolites formed in incubations were quantified by LC with radiometric detection (method A) as described in Section 2.7.

3.5.1. Kinetics of enzymatic metabolism of ^{14}C-LAS34823 and ^{14}C-LAS34850

The kinetics of ^{14}C-LAS34823 metabolism was investigated in pooled human liver microsomes over the concentration range 0.5–500 μM. A single radioactive metabolite M1 was observed in all the radiochromatograms (Fig. 3). The kinetic profile of M1 formation exhibited substrate inhibition at LAS34823 concentrations greater than 100 μM, indicating that LAS34823 may inhibit its own metabolism (Fig. 7A). Unfortunately, experimental data could not be fitted to any substrate inhibition model due to the severity of the inhibition. Within LAS34823 concentration range between 2 and 100 μM, the Eadie–Hofstee plot of the kinetic data obtained exhibited a biphasic pattern, suggesting that two enzymes of different affinity could be involved in the formation of M1 (Fig. 7A). Although limited experimental data were available, data fitting was carried out assuming a bi-enzymatic Michaelis–Menten model within this concentration range. The high-affinity component exhibited apparent K_{m1} and V_{max1} values of 2.1 μM and 20.1 pmol/min/mg protein, respectively. The low-affinity component exhibited apparent K_{m2} and V_{max2} values of 65.5 μM and 192.7 pmol/min/mg protein, respectively. The catalytic efficiency (V_{max}/K_m) of the high-affinity component was approximately three-fold higher than that observed for the low-affinity component (Table 4).

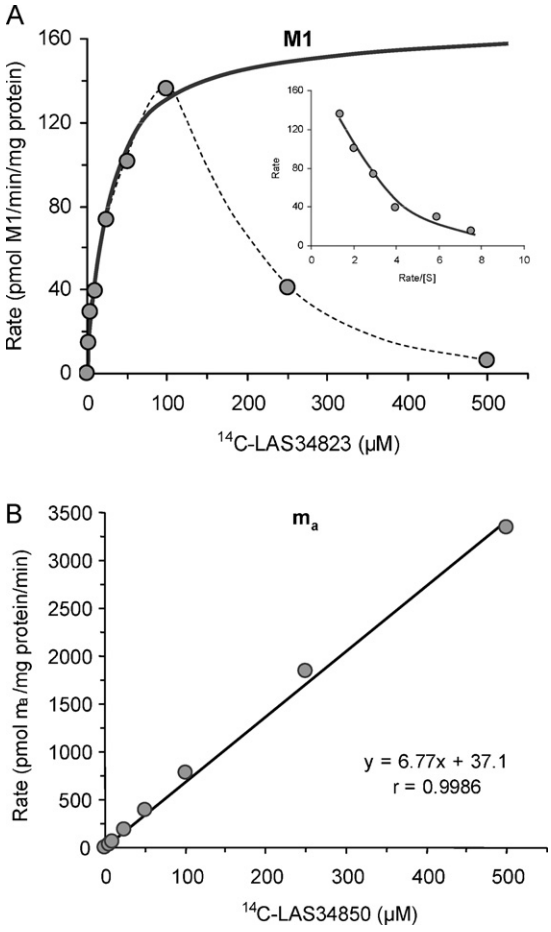

Fig. 7. Kinetics of (A) M1 formation from ^{14}C-LAS34823, and (B) m_a formation from ^{14}C-LAS34850 in human liver microsomes. Symbols represent observed data (mean of duplicate determinations). Solid lines represent calculated rates with (A) bi-enzymatic Michaelis–Menten equation in the range of concentration of 2–100 μM and (B) linear regression.

On the other hand, following incubations of ^{14}C-LAS34850 with liver microsomes, the formation of the radioactive peak m_a was observed in phosphate buffer and liver microsomes only in the presence of NADPH-generating system or reduced NADPH, but not with $NADP^+$ (oxidized form). The fact that liver microsomal protein was not essential for m_a formation strongly suggests a non-enzymatic reaction. Furthermore, the kinetics of ^{14}C-LAS34850 metabolism was investigated in pooled human liver microsomes over the concentration range 0.5–500 μM in the presence of NADPH-generating system. No other LAS34850 metabolites apart from m_a were observed at any concentration and the time course of m_a formation was linear with increasing LAS34850 concentrations, confirming that its formation was non-enzymatic and only NADPH-dependent (Fig. 7B).

3.5.2. Kinetics of enzymatic metabolism of ^{14}C-phe-AB

The esterase-mediated hydrolysis of ^{14}C-phe-AB (5 μM) in human liver microsomes (1 and 2 mg/ml) was investigated in the absence of NADPH. Parallel incubations in buffer (pH 7.4) were also carried out as a control of non-enzymatic hydrolysis. There were slight differences in the formation of LAS34823 between human

Table 4
Apparent kinetic parameters for the oxidative metabolism of ^{14}C-LAS34823, ^{14}C-phe-AB and ^{14}C-glyc-AB. Test compounds (0.5–100 μM ^{14}C-phe-AB and 2–100 μM ^{14}C-LAS34823) were incubated in phosphate buffer (pH 7.4) and with human liver microsomes in the presence and absence of NADPH.

Metabolite	Test compound	System	K_m (μM)	V_{max} (pmol/min/mg protein)	Cl_{int} (μl/min/mg protein)	K_h (min^{-1})
M1	^{14}C-LAS34823	HLM + NADPH	K_{m1} 2.1 K_{m2} 65.5	V_{max1} 20.1 V_{max2} 192.7	9.6 2.9	NA NA
M2	^{14}C-phe-AB	Buffer	–	–	–	0.014
		HLM–NADPH	0.43	37.7	87.7	0.012
		HLM + NADPH	1.78	253.9	142.8	0.010
M3/m4	^{14}C-phe-AB	HLM + NADPH	22.6	283.4	12.5	NA
	^{14}C-glyc-AB	HLM + NADPH	18.3	229.2	12.6	NA
M4/m5	^{14}C-phe-AB	HLM + NADPH	4.6	106.0	23.0	NA
	^{14}C-glyc-AB	HLM + NADPH	5.8	100.4	17.4	NA
m2	^{14}C-glyc-AB	HLM + NADPH	0.4	328.3	812.5	0.022

NA, not applicable.

liver microsomes and the incubation buffer. In fact, the net enzymatic hydrolysis of aclidinium at a microsomal protein concentration of 2 mg/ml was less than 20% after 60 min of incubation. These results suggest that the esterase(s) responsible for the aclidinium hydrolysis have low catalytic activity in human liver microsomes.

In terms of substrate depletion, the rapid non-enzymatic hydrolysis of aclidinium compromised the selection of the incubation time for further kinetic studies. Incubation times of above 15 min led to a substrate depletion higher than 20%.

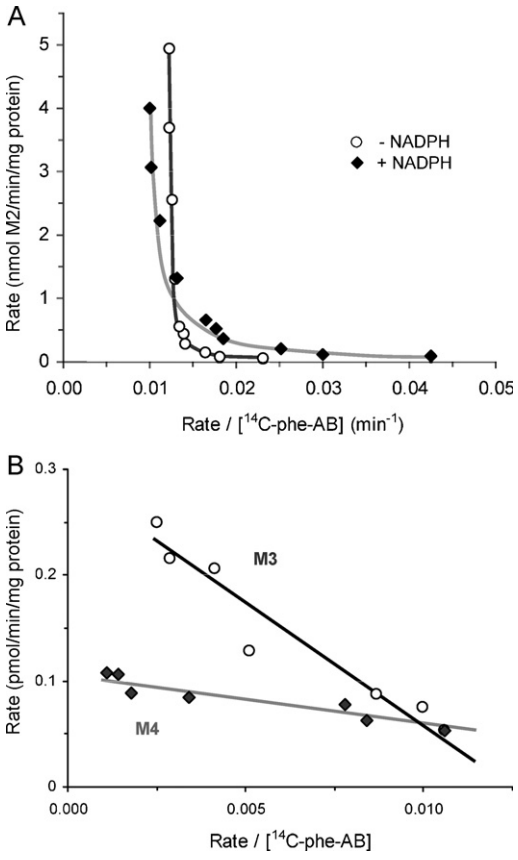

Fig. 8. Eadie–Hofstee plots of (A) M2 formation from ^{14}C-phe-AB with (filled diamonds) and without (open circles) NADPH and (B) M3 and M4 formation from ^{14}C-phe-AB in human liver microsomes. Symbols represent observed data (mean of duplicate determinations); solid lines represent rates calculated by non-linear regression.

Moreover, at the highest protein concentration assayed (1 mg/ml) and incubation times of 15 and 30 min, aclidinium disappearance was also considerable due to the enzymatic formation of the oxidative metabolites M3 and M4. As a compromise, an incubation time of 15 min and 0.25 mg of microsomal protein/ml was selected.

The inhibitory potential of the main hydrolysis metabolites towards human esterases was of low relevance [4]. In addition, human CYP1A2, 2A6, 2C8, 2C9, 2C19, 2D6, 2E1, 3A4/5, and A9/11 activities were not inhibited by LAS34850 in vitro, whereas CYP2D6 was inhibited competitively by LAS34823 with an inhibition constant of 15.5 μM [11]. Thus, taking into account all these data, any potential interference of the hydrolysis metabolites on the characterization of the kinetics of ^{14}C-phe-AB and ^{14}C-glyc-AB is very unlikely.

The kinetics of ^{14}C-phe-AB metabolism was investigated in pooled human liver microsomes over the concentration range 0.5–100 μM. In parallel, ^{14}C-phe-AB was also incubated in phosphate buffer and with human liver microsomes without NADPH-generating system. The K_h in the incubation buffer was calculated from the slope of the regression line (r^2 = 0.9991) and presented a value of 0.014 min^{-1} (Table 4). The major metabolite was M2 (LAS34823) and following inspection of the Eadie–Hofstee plot obtained in human liver microsomes, two different phases could clearly be differentiated (Fig. 8A). At low aclidinium concentrations, enzymatic hydrolysis may occur via esterases, and it was assumed that this process could be well described using the typical Michaelis–Menten equation. However, non-enzymatic hydrolysis becomes predominant at high substrate concentrations, leading to a constant value of the $v/[S]$ ratio, which is represented by the non-enzymatic hydrolysis rate constant (K_h). The kinetic parameters were calculated using the mixed model described above (Section 2.10). The formation of M2 (LAS34823) without NADPH exhibited apparent K_m and V_{max} values of 0.43 μM and 37.7 pmol/min/mg protein, respectively. In contrast, higher apparent K_m and V_{max} values (1.78 μM and 253.9 pmol/min/mg protein, respectively) were obtained in the presence of NADPH. The apparent K_h values of ^{14}C-phe-AB in human liver microsomes with and without NADPH were 0.012 and 0.010 min^{-1}, respectively. The calculated intrinsic clearance (V_{max}/K_m) with and without NADPH was 87.7 and 142.8 μl/min/mg protein, respectively, which is consistent with an additional NADPH-dependent metabolism of AB apart from enzymatic hydrolysis.

The formation of the minor metabolites M3 and M4 was only observed in the presence of human liver microsomes and NADPH-generating system, confirming that their formation was enzymatic and NADPH-dependent. The kinetics of the formation of metabolites M3 and M4 followed the Michaelis–Menten model (Fig. 8B).

The formation of M3 exhibited apparent K_m and V_{max} values of 22.6 μM and 283.4 pmol/min/mg protein, respectively. The formation of M4 exhibited apparent K_m and V_{max} values of 4.6 μM and 106 pmol/min/mg protein, respectively. The enzymatic intrinsic clearance values (Cl_{int}) for M3 and M4 were 12.5 and 23.0 μl/mg protein/min, respectively (Table 4).

3.5.3. Kinetics of enzymatic metabolism of ^{14}C-glyc-AB

The formation of ^{14}C-glyc-AB metabolites in human liver microsomes was conducted in the incubation conditions established for ^{14}C-phe-AB. Parallel incubations were also conducted in the incubation buffer as a control of non-enzymatic hydrolysis. The principal metabolite was the hydrolysis metabolite m3 (LAS34850) and was generated non-enzymatically as described above. Thus, m3 formation was linear in incubation buffer and a similar profile was also obtained in liver microsomes without NADPH. Interestingly, m3 (LAS34850) formation was lower after incubation in human liver microsomes with NADPH. This was a general observation for all concentrations tested (Fig. 9A). As an example, the rates of formation at a ^{14}C-glyc-AB concentration of 5 μM were 253 and 171 pmol/min/mg protein, without and with NADPH, respectively.

The formation of m2 in incubations with human liver microsomes and NADPH followed a clear biphasic kinetic profile, which is in agreement with the participation of at least two different processes in its formation (Fig. 9B). Following visual inspection of the Eadie–Hofstee plot and the standard errors of calculated parameters, the profile was best fitted to a mixed model assuming non-enzymatic degradation as well as to an enzymatic process (Michaelis–Menten), as described above. Assuming this model, the apparent hydrolysis rate constant K_h was very rapid (0.022 ± 0.002 min^{-1}), representing a half-life of 32 min. The apparent K_m and V_{max} were 0.40 μM and 328.3 pmol/mg protein/min, respectively. The intrinsic clearance was calculated to be 812.5 μl/min/mg protein. The formation of m4 was enzymatic and NADPH-dependent. Its formation followed Michaelis–Menten kinetics with K_m and V_{max} values of 18.3 μM and 229.2 pmol/min/mg protein, respectively, which are practically identical to those found for M3 after incubation of ^{14}C-phe-AB, confirming that M3 and m4 are actually the same metabolite. The generation of metabolite m5 was also enzymatic and NADPH-dependent. The apparent Michaelis–Menten parameters K_m and V_{max} were 5.8 μM and 100.4 pmol/min/mg protein, respectively, also similar to those found for M4 (Table 4).

The formation of m_a was only observed at high ^{14}C-glyc-AB concentrations and required the presence of a NADPH-generating system, as already described for LAS34850. The formation of metabolites m1 and m5 was negligible, thus, precluding any attempt of identification.

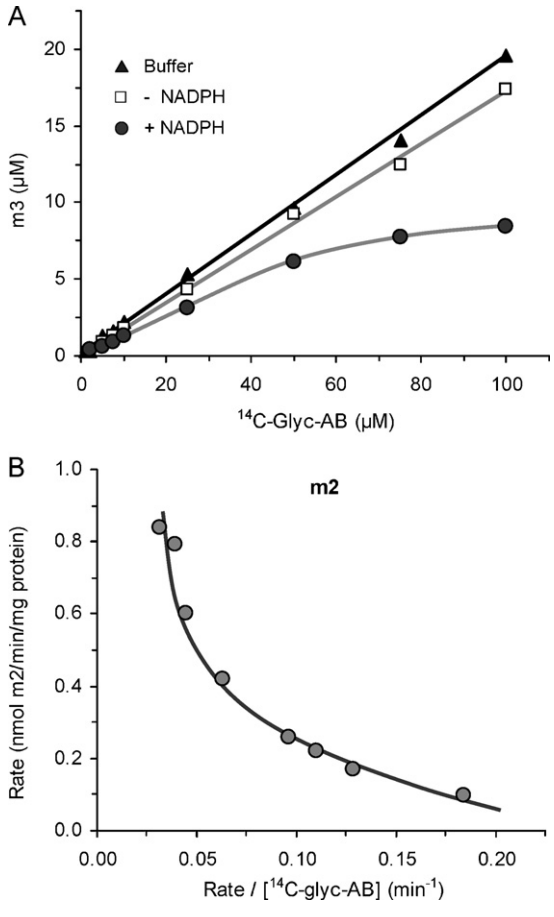

Fig. 9. (A) Formation of metabolite m3 (LAS34850) from ^{14}C-glyc-AB in incubation buffer (filled triangles), human liver microsomes without NADPH, and human liver microsomes with NADPH. (B) Eadie–Hofstee plot of m2 from ^{14}C-glyc-AB in human liver microsomes. Symbols represent observed data (mean of duplicate determinations); solid lines represent rates calculated by non-linear regression.

3.6. Identification of P450 isoforms responsible for the metabolism of ^{14}C-phe-AB and ^{14}C-glyc-AB

The identification of the P450 enzymes responsible for the formation of the oxidative metabolites of ^{14}C-LAS34823, ^{14}C-LAS34850, ^{14}C-phe-AB, and ^{14}C-glyc-AB was conducted using three different approaches: (a) incubations of test compounds with commercially available human cDNA-expressed P450 and FMO isoenzymes, (b) effect of selective chemical inhibitors of P450 isoenzymes in human liver microsomes, and (c) effect of selective antibodies against P450 isoenzymes in human liver microsomes.

3.6.1. Identification of P450 isoforms responsible for the ^{14}C-LAS34823 metabolism

The incubations of ^{14}C-LAS34823 with human recombinant P450 (25 pmol/ml) and FMO (0.2 mg/ml) isoforms were carried out at a LAS34823 concentration of 5 μM. The formation of M1 was catalyzed only by human recombinant CYP2D6 with practically complete conversion of LAS34823 into M1. Additional metabolites were not observed in the presence of other P450 isoforms or flavin-containing monooxygenases (FMO1, FMO3, and FMO5). The kinetic parameters of M1 formation in the presence of recombinant human CYP2D6 were determined, corrected by P450 content (2 pmol/ml) and incubation time (20 min), in order to ensure linear conditions and low substrate depletion. An important inhibitory effect on M1 formation was observed at substrate concentrations above 5 μM and complete inhibition was obtained at the highest LAS34823 concentrations assayed (100–200 μM). Within the LAS34823 concentration range 0.5–5 μM, the formation of M1 by CYP2D6 followed Michaelis–Menten kinetics with apparent K_m and V_{max} values of 4.9 μM and 22.1 pmol/min/pmol P450, respectively. These results are in agreement with the high-affinity enzyme observed in human liver microsomes (Section 3.5.1). Incubations at higher LAS34823 concentrations to identify the possible low-affinity component observed in human liver microsomes were not conducted, as it was not considered relevant due to the low systemic LAS34823 concentrations (<0.5 nM) observed in clinical trials [12]. Following incubation in the presence of different chemical and antibody inhibitors, the formation of M1 was strongly inhibited by quinidine (CYP2D6 inhibitor) and by the antibody against CYP2D6 (Table 5).

Table 5
Summary of in vitro human P450 reaction phenotyping of aclidinium bromide metabolism obtained in recombinant human P450 isoforms and human liver microsomes.

Metabolite	Substrate	Recombinant human P450 isoforms (*n*-fold basal activity)	Inhibition (%)	
			Chemical	Antibody
m1	^{14}C-glyc-AB	–	No effect	No effect
m2	^{14}C-glyc-AB	↑ 2D6 (≈2.6-fold at 5 and 25 μM) ↑ 3A4 (≈1.4-fold at 5 and 25 μM)	Ketoconazole: 58% Quercetin: 25%	CYP3A4: 52%
M1	^{14}C-LAS34823	↑ 2D6 (>40-fold)	Quinidine: >80%	CYP2D6: >80%
	^{14}C-phe-AB	↑ 2D6 (>4.3-fold)	–	–
M2	^{14}C-phe-AB	↑ 2D6 (2.2-fold at 5 μM)	Ketoconazole: 28%	CYP3A4: 23%
m3	^{14}C-glyc-AB	↓ 2D6 (0.7-fold at 5 μM)	No effect	No effect
m_a	^{14}C-glyc-AB	No effect	–	–
M3/m4	^{14}C-phe-AB	–	Ketoconazole: >77% Quercetin: 44% Quinidine: 20%	CYP3A4: >70% CYP2D6: 31%
	^{14}C-glyc-AB	–	Ketoconazole: >35%	CYP2D6: 34% CYP3A4: 32%
M4/m5	^{14}C-phe-AB	↑ 2D6 (>6.5-fold)	Quinidine: >77%	CYP2D6: 62%
	^{14}C-glyc-AB	↑ 2D6 (>1.6-fold at 5 μM, >3.2-fold at 25 μM) ↑ 1A1 (>1.8-fold at 25 μM)	Quinidine: >48%	CYP2D6: 40%

See Sections 2.5 and 2.6 for incubation details.
–: Metabolite not detected at any of the concentrations assayed.
M5/m6 and M6/m7 were not detected in the experiments.
↑/↓: increased/decreased activity with human recombinant CYP compared to control incubation (insect control). The remaining human rCYPs did not have any influence on metabolite formation.
No effect: enzyme activity was not significantly inhibited (<20% inhibition) against control incubations.

3.6.2. Identification of P450 isoforms responsible for the ^{14}C-phe-AB metabolism

The incubation of ^{14}C-phe-AB (5 μM) with human P450 (25 pmol/ml) and FMO (0.2 mg/ml) isoforms revealed that the formation of M1 (hydroxylated LAS34823) and M4 was only catalyzed by CYP2D6. Remarkably, the rate of formation of M2 (LAS34823) was also higher with human rCYP2D6 (2.92 pmol/min/pmol CYP) compared to the other rCYP isoforms (1.3–1.5 pmol/min/pmol CYP). Unfortunately, metabolite M3 was not observed in the incubation samples at the assay concentrations. Therefore, further inhibition experiments with chemical P450 inhibitors and antibodies in liver microsomes were studied at a ^{14}C-phe-AB concentration of 25 μM. At this concentration, the formation of M2 was slightly inhibited (28%) by the presence of ketoconazole (CYP3A4 inhibitor) and the formation of M3 was decreased by ketoconazole and slightly by quinidine. The formation of M4 was catalyzed by human rCYP2D6 and totally blocked by quinidine in human liver microsomes. Interestingly, human CYP1A1, which appears to be expressed in human liver at low levels [13,14], could be also involved in the formation of M4. This means that the oxidative metabolism in the human lungs from smokers could be increased, since smoking-induced elevated levels of CYP1A1 have been observed [15].

The remaining chemical inhibitors had no particular influence on ^{14}C-phe-AB metabolism. These results were also confirmed in the studies conducted with selective P450 antibodies. M2 formation was slightly affected by the presence of anti-CYP3A4, whilst M3 and M4 formation were inhibited by CYP3A4 and CYP2D6 inhibitory antibodies, respectively (Table 5).

3.6.3. Identification of P450 isoforms responsible for the ^{14}C-glyc-AB metabolism

Incubations of ^{14}C-glyc-AB with recombinant human P450 isoforms (rP450) were conducted at two different substrate concentrations (5 and 25 μM), in order to monitor the metabolite formation adequately. Further studies on the effect of different P450 chemical inhibitors and antibodies were studied at a single ^{14}C-glyc-AB concentration of 25 μM. The results of these studies are summarized in Table 5.

The formation of the hydrolysis metabolite m3 (LAS34850) was similar for all rCYPs assayed and control incubations (approximately 12 pmol/min/pmol CYP), except in the case of CYP2D6, where a slight reduction was observed (9.5 pmol/min/pmol CYP). Metabolite m3 formation was not significantly affected by any of the human P450 inhibitors and inhibitory antibodies, indicating that its formation was not P450-dependent.

Metabolite m1 was not observed in the presence of any of the rCYP isoforms assayed, most probably because the formation of this metabolite is dependent on m2 and/or m4 concentrations, which were always low. Metabolite m2 was formed to a similar extent in insect control incubations and with most human rCYPs (approx. 0.38 and 1.00 pmol/min/pmol CYP at 5 and 25 μM, respectively), with the exception of human CYP2D6 (1.02 pmol/min/pmol CYP at 5 μM and 2.5 pmol/min/pmol CYP at 25 μM) and CYP3A4 (0.49 pmol/min/pmol CYP at 5 μM and 1.40 pmol/min/pmol CYP at 25 μM), suggesting that these enzymes may be involved in its formation. The formation of m2 was inhibited substantially by ketoconazole (CYP3A4 inhibitor) and slightly by quercetin (CYP2C8 inhibitor). Moreover, the formation of m2 in human liver microsomes was slightly affected by the presence of CYP3A4 antibodies. Metabolite m_a was observed to a similar extent in incubations with insect control and human rP450 isoforms (from 0.8 to 1.3 pmol/min/pmol CYP), which is in accordance with the formation of LAS34850 and further chemical reduction by NADPH, because this co-factor was always present in the incubations. The formation of metabolite m4 was not catalyzed by any human CYP isoform at the two different substrate concentrations, although these results should be taken with caution due to the similar retention times of metabolites m4 and m_a. Curiously, metabolite m4 was not observed in incubations with recombinant CYP isoforms at any of the concentrations of ^{14}C-glyc-AB assayed. In contrast, m4 was detected in inhibition studies with human liver microsomes. In these studies, some degree of inhibition was observed in the presence of human CYP3A4 and 2D6 antibodies, although conclusive results could not be obtained due to the low activity observed.

The formation of the hydroxylated metabolite m5 (M4) was mainly catalyzed by CYP2D6 (1.08 pmol/min/pmol CYP at 25 μM), as observed in ^{14}C-phe-AB incubations. This metabolite was also

formed to a lesser extent in the presence of enzyme CYP1A1 (0.60 pmol/min/pmol CYP at 25 μM). CYP1A1 involvement in the formation of M4 was not observed after ^{14}C-phe-AB incubation, most probably due to the low concentration assayed (5 μM). Metabolite m5 formation in human liver microsomes was inhibited only by quinidine (CYP2D6 inhibitor) and human CYP2D6 antibodies, which is in agreement with the results obtained above (Table 5).

4. Discussion

The non-enzymatic hydrolysis of aclidinium bromide (AB) observed in the incubation buffer (pH 7.4) was high and accounted for approximately 45% of overall metabolism in incubations conducted with liver microsomes. The rate of enzymatic hydrolysis of both radiolabeled forms, measured in the absence of NADPH, was higher in of rabbits and dogs, followed by mice. Remarkably, the formation rate of the hydrolysis metabolites in rat and human liver microsomes was similar to that obtained in buffer incubation, suggesting a low esterase activity in these liver subcellular fractions. This observation has already been done in a previous study using human liver microsomes [4].

The net oxidative metabolism obtained by subtraction of non-NADPH and NADPH-dependent metabolism was similar across all species examined, but its extent was far lower compared to the hydrolysis process. In hepatocytes, the overall rate of aclidinium metabolism followed the rank order: rabbit > mouse > dog > rat ≈ human. Although the enzymatic hydrolysis of aclidinium in hepatocytes cannot be differentiated from its overall metabolism, the metabolism pattern was similar to the obtained in liver microsomes.

The major radioactive metabolites of ^{14}C-phe-AB and ^{14}C-glyc-AB detected in liver microsomes and hepatocytes of all species were the alcohol and acid metabolites, M2 (LAS34823) and m3 (LAS34850), respectively. These two hydrolysis metabolites are devoid of in vitro antimuscarinic activity and show no relevant bronchodilatory activity in preclinical models [3].

The formation of M2 (LAS34823) was slightly higher in human liver microsomes with NADPH at low ^{14}C-phe-AB concentrations. Inspection of Eadie–Hofstee plots confirmed the differentiation between enzymatic and non-enzymatic hydrolysis, as previously observed in human plasma [4]. The slight inhibition of LAS34823 formation produced by ketoconazole and CYP3A4 antibody may be explained by the inhibition of the precursor metabolite M3/m4, the formation of which was also mediated by CYP3A4. In contrast, m3 formation (LAS34850) was lower after incubation in human liver microsomes with NADPH, which could be related to the increased oxidative pathway of primary metabolites such as M3/m4, whose hydrolysis leads to the formation of metabolites other than m3. On the other hand, m3 formation was similar with all recombinant CYPs assayed with the exception of CYP2D6, where small amounts were formed. This fact confirms that other metabolic routes involving the thiopheneglyoxylic moiety of aclidinium are in competition with the hydrolysis process.

Other major metabolites obtained in incubations of ^{14}C-phe-AB and ^{14}C-glyc-AB were identified as hydroxylated LAS34823 (M1) and 2-thiopheneglyoxylic acid (m2), respectively.

In humans, the formation of M1 from LAS34823 was catalyzed by CYP2D6 and a substrate inhibition profile was apparent at higher concentrations, which is in agreement with a previous in vitro study where this compound was shown to be a moderate inhibitor of the catalytic activity of human CYP2D6 with an apparent K_i of 15 μM [11]. Following incubation of AB, the formation of M1 could be explained by two different routes: (a) direct hydroxylation of the hydrolysis product LAS34823 (M2) and (b) hydrolysis of metabolite M4/m5.

The rapid generation of m2 in liver microsomes and hepatocytes is difficult to interpret. According to its chemical structure, the most plausible explanation for its formation is related to the primary oxidation of m4/M3 and further hydrolysis, as represented in Fig. 1. Indeed, the formation of m2 followed a biphasic kinetic profile in incubations with human liver microsomes and NADPH, consistent with the participation of two different processes (Fig. 9B).

The apparent K_h obtained for m2 was higher than that observed for the hydrolysis metabolite M2, suggesting a faster hydrolysis of its tentative primary metabolite M_f into m2 and M2 (LAS34823). Furthermore, the enzymatic origin of m2 was demonstrated by its formation in the presence of rCYP2D6 and in lower amounts by rCYP3A4. The involvement of CYP2D6 and CYP3A4 was further confirmed by inhibition studies. The fact that m2 formation was more affected by CYP3A4 inhibitors could be explained by the relative content of these enzymes in the human liver, with average values of 30% (CYP3A4) and 2.5% (CYP2D6) of the total P450 content [16]. The slight inhibition caused by quercetin could be explained by its lack of selectivity as a CYP2C8 inhibitor, as described by Obach [17]. The low apparent K_m and the high intrinsic clearance suggest that this metabolic pathway would be relevant in vivo.

The minor aclidinium metabolites M3/m4, M4/m5, M5/m6, M6/m7, and m1 accounted for less than 5% of total metabolism in liver microsomes and were not detected in hepatocytes, suggesting that these metabolites are actually intermediate metabolites that are likely to be further metabolized. As it was expected, the formation of these intermediate metabolites was similar following incubations of ^{14}C-phe-AB and ^{14}C-glyc-AB with liver microsomes. The origin of metabolite M3/m4 is an intriguing issue that cannot be completely addressed for the moment. However, the loss of a thiophene ring from aclidinium could be explained by thiophene oxidation (hydroxylation or S-oxidation) and further ring opening in a similar manner that has been described for compounds such as suprofen and tienilic acid [18]. This complex process would mean that the minor metabolites M5/m6 and M6/m7 could actually be precursors for the formation of M3/m4. An interesting observation was that the primary metabolite M3/m4 was generated to a greater extent than its oxidized metabolite M_f, which was only detected by MS. In contrast, the metabolite m2 (hydrolytic metabolite of M_f) was always formed to a greater extent than m1 (hydrolytic metabolite of M3/m4), strongly supporting faster hydrolysis of the primary metabolite M_f compared to M3/m4. The formation of the p-hydroxylated metabolite of aclidinium (M4/m5) was catalyzed by human CYP2D6, in analogy to the formation of M1. Metabolite m1 (hydroxyl-2-thienylacetic acid) was observed at very low levels in liver microsomes of mouse, rabbit, and human, which could be associated with the hydrolysis of its primary metabolite M3/m4. In this study, one of the minor metabolic routes identified involved the oxidation of the thiophene rings of aclidinium (M5/m6 and M6/m7). The formation of these metabolites could be related to the formation of potential reactive metabolites. However, the recovery of total radioactivity in the supernatans of incubations of ^{14}C-phe-AB, ^{14}C-glyc-AB, ^{14}C-LAS34823, and ^{14}C-LAS34850 in human liver microsomes was greater than 85%, which suggests that this metabolic route would be a minor process. Additional investigations were also performed although the results of these studies are outside the scope of the current study.

The incubation of ^{14}C-LAS34850 in human liver microsomes revealed some interesting features. An artifact was generated in the incubation buffer that was identified as the compound di-2-thienyl ketone. The biomimetic oxidative formation of a similar compound has been also described for denaverine hydrochloride [19]. The formation of metabolite m_a was only observed in incubations where the NADPH (reduced form) was present with or

without liver microsomes, which would be compatible with a non-enzymatic reduction process of the hydroxyl moiety by NADPH. Furthermore, the formation of m_a was linear with increasing LAS34850 concentrations, confirming that its formation was non-enzymatic. On the other hand, it is important to note that the polar metabolites m1 and m2 were not generated during the incubation of ^{14}C-LAS34850 with human liver microsomes and hepatocytes. These observations confirm that these metabolites can be formed only from the parent compound but not from m3 (LAS34850), which is the main circulating metabolite in humans [12].

In summary, the present study indicates that aclidinium hydrolysis is the main biotransformation route in liver microsomes and hepatocytes of mouse, rat, rabbit, dog, and human, with rabbit and dog exhibiting the highest rates of enzymatic hydrolysis. Oxidative metabolism in liver microsomes and hepatocytes was substantially lower when compared to ester hydrolysis. The metabolite profiles were similar across all five species examined and up to five primary metabolites and eight secondary metabolites were characterized. The alcohol metabolite (LAS34823) is transformed to a single hydroxylated metabolite that is subsequently glucuronidated. In contrast, the acid metabolite (LAS34850) was not metabolized enzymatically in vitro. The oxidative conversion of AB and its alcohol metabolite was primarily catalyzed by human CYP3A4 and CYP2D6, respectively.

Acknowledgments

We would like to acknowledge the technical support provided by Francisco Jimenez Berbell. We also thank Josep M. Huerta, Department of Computational and Structural Drug Discovery (Almirall, S.A.), for analyzing the ^{1}H NMR spectrum of metabolite M1.

References

[1] Gavaldà A, Miralpeix M, Ramos I, Otal R, Carreño C, Viñals M, et al. Characterization of aclidinium bromide, a novel inhaled muscarinic antagonist, with long duration of action and a favorable pharmacological profile. J Pharmacol Exp Ther 2009;331:740–51.

[2] Prat M, Fernández D, Buil MA, Crespo MI, Casals G, Ferrer M, et al. Discovery of novel quaternary ammonium derivatives of (3R)-quinuclidinol esters as potent and long-acting muscarinic antagonists with potential for minimal systemic exposure after inhaled administration: identification of (3R)-3-{[hydroxy(di-2-thienyl)acetyl]oxy}-1-(3-phenoxypropyl)-1-azoniabicyclo[2.2.2]octane bromide (aclidinium bromide). J Med Chem 2009;52:5076–92.

[3] Sentellas S, Ramos I, Albertí J, Salvà M, Antón F, Miralpeix M, et al. Aclidinium bromide, a new, long-acting, inhaled muscarinic antagonist: in vitro plasma inactivation and pharmacological activity of its main metabolites. Eur J Pharm Sci 2010;39:283–90.

[4] Albertí J, Martinet A, Sentellas S, Salvà M. Identification of the human enzymes responsible for the enzymatic hydrolysis of aclidinium bromide. Drug Metab Disp 2010;38:1202–10.

[5] Placidi L, Scott EC, de Sousa G, Rahmani R, Placidi M, Sommadossi JP. Interspecies variability of TNP-470 metabolism, using primary monkey, rat, and dog cultured hepatocytes. Drug Metab Dispos 1997;25:94–9.

[6] Hewitt NJ, Fischer T, Zuehlke U, Oesch F, Utesch D. Metabolic activity of fresh and cryopreserved cynomolgus monkey (*Macaca fascicularis*) hepatocytes. Xenobiotica 2000;30:665–81.

[7] Bednár P, Lemr K, Barták P, Sevcík J, Hlavác J, Stýskala J, et al. Capillary electrophoresis/mass spectrometry: a promising tool for the control of some physiologically hazardous compounds. I-derivatives of 3-quinuclidinol. J Mass Spectrom 2002;37:1213–8.

[8] Pati S, Losito I, Palmisano F, Zambonin PG. Characterization of caffeic acid enzymatic oxidation by-products by liquid chromatography coupled to electrospray ionization tandem mass spectrometry. J Chromatogr A 2006;1102:184–92.

[9] Ma YC, Kim HY. Determination of steroids by liquid chromatography/mass spectrometry. J Am Soc Mass Spectrom 1997;8:1010–20.

[10] Volmer DA, Hui JPM. Rapid determination of corticosteroids in urine by combined solid phase microextraction/liquid chromatography/mass spectrometry. Rapid Commun Mass Spectrom 1997;11:1926–33.

[11] Almirall SA, data on file.

[12] Jansat JM, Lamarca R, García-Gil E, Ferrer O. Safety and pharmacokinetics of single doses of aclidinium bromide, a novel long-acting, inhaled muscarinic, in healthy subjects. J Clin Pharmacol Ther 2009;47:460–8.

[13] Stiborová M, Martínek V, Rýdlová H, Hodek P, Frei E, Sudan I. Is a potential carcinogen for humans: evidence for its metabolic activation and etoxication by human recombinant cytochrome P450 1A1 and liver microsomes. Cancer Res 2002;62:5678–84.

[14] Drahushuk AT, McGarrigle BP, Larsen KE, Stegeman JJ, Olson JR. Detection of CYP1A1 protein in human liver and induction by TCDD in precision-cut liver slices incubated in dynamic organ culture. Carcinogenesis 1998;19:1361–8.

[15] Smith GBJ, Harper PA, Wong JMY, Lam MSM, Reid KR, Petsikas D, et al. Human lung microsomal cytochrome P4501A1 (CYP1A1) activities. Impact of smoking status and CYP1A1, Aryl hydrocarbon receptor, and glutathione S-transferase M1 genetic polymorphisms. Cancer Epidemiol Biomarkers Prev 2001;10:839–53.

[16] Rendic S, DiCarlo FJ. Human cythocrome P450 enzymes: a status report summarizing their reactions, substrates, inducers and inhibitors. Drug Metab Rev 1997;29:413–580.

[17] Obach R. Inhibition of human cytochrome P450 enzymes by constituents of St. John's Wort, an herbal preparation used in the treatment of depression. J Pharmacol Exp Ther 2000;294:88–95.

[18] O'Donnell JP, Dalvie DK, Kalgutkar AS, Obach RS. Mechanism-based inactivation of human recombinant P450 2C9 by the nonsteroidal anti-inflammatory drug suprofen. Drug Metab Dispos 2003;31:1369–77.

[19] Smolinka K, Göber B. Biomimetic oxidation of denaverine hydrochloride. Eur J Org Chem 1999;3:679–83.